NMR Experiments for the Measurement of Carbon Relaxation Properties in Highly Enriched, Uniformly $^{13}C,^{15}N$-Labeled Proteins: Application to $^{13}C^{\alpha}$ Carbons

Toshio Yamazaki, Ranjith Muhandiram, and Lewis E. Kay*

Contribution from the Protein Engineering Network Centers of Excellence and Departments of Medical Genetics, Biochemistry and Chemistry, Medical Sciences Building, University of Toronto, Toronto, Ontario, Canada M5S 1A8

Received February 2, 1994®

Abstract: New two-dimensional NMR experiments with high sensitivity and resolution are presented for the measurement of T_1, $T_{1\rho}$, and steady-state $^1H-^{13}C$ NOE values for CH $^{13}C^{\alpha}$ spin systems in highly enriched, uniformly ^{13}C-labeled proteins. Using a sample consisting of approximately equimolar amounts of 99% $^{13}C^{\alpha}$-alanine and 99% uniformly ^{13}C-labeled alanine ($^{13}C_3$-alanine) dissolved in perdeuterated glycerol, high signal-to-noise $^{13}C^{\alpha}$ relaxation measurements of both singly and uniformly ^{13}C-labeled alanine have been made. This allows an investigation of the influence of both carbon-carbon scalar coupling effects and dipolar relaxation effects on the measurement of relaxation properties of carbon spins. T_1, $T_{1\rho}$, and steady-state $^1H^{\alpha}-^{13}C^{\alpha}$ NOE values have been measured over a range of temperatures from 10 °C to 40 °C, with the correlation time for molecular tumbling varying from ~17 to ~1 ns. The results indicate that, for macromolecules, the contributions to the longitudinal carbon relaxation from neighboring carbons must be included in the interpretation of T_1 data in terms of motional models. The $^1H^{\alpha}-^{13}C^{\alpha}$ steady-state NOE can be influenced significantly by $^{13}C^{\alpha}-^{13}C^{\beta}$ cross relaxation, and because of the small $^1H^{\alpha}-^{13}C^{\alpha}$ NOE in proteins, it may not be possible to measure $^1H^{\alpha}-^{13}C^{\alpha}$ NOE values with high accuracy. Theoretical results are presented which indicate that it is possible to measure accurate $^{13}C^{\alpha}$ $T_{1\rho}$ values in all residues, with the exception of serine and threonine when the $^{13}C^{\alpha}$ and $^{13}C^{\beta}$ chemical shifts are nearly equivalent, and experimental verification is provided for the case of alanine. A strategy is proposed for obtaining accurate dynamics of $^{13}C^{\alpha}$ carbons based on the measurement of $^{13}C^{\alpha}$ T_1 values using at least two field strengths and $T_{1\rho}$ values measured at a single field.

Introduction

Recent developments in multinuclear, three- and four-dimensional NMR methods have increased the molecular weight limits of protein structure determination and have improved the precision and accuracy of NMR-derived structures.[1-4] Present efforts in the field have been particularly focused on the generation of time-averaged "static" three-dimensional protein structures; however, it is well recognized that a complete description of the structure of a protein requires knowledge of motional properties as well.[5,6] NMR is particularly well suited for this, in that the same processes which give rise to the appearance of NOE cross peaks used for distance information in protein structure determination can also be exploited to obtain dynamic information. A significant number of studies have appeared in the literature in the past few years describing the backbone dynamics of a wide variety of uniformly ^{15}N-labeled proteins based on measurements of ^{15}N T_1 and T_2 relaxation times as well as steady-state $^1H-^{15}N$ NOE values.[7-12] The resolving power of two-dimensional spectroscopy coupled with the high sensitivity of the ^{15}N relaxation experiments allows the measurement of backbone dynamics at virtually every backbone ^{15}N position in the molecule. A number of ^{13}C relaxation studies at natural abundance or on samples labeled with ^{13}C at specific sites have also been published.[13-17] The use of ^{13}C spectroscopy to probe protein dynamics is particularly appealing in that both backbone and side-chain motions can be characterized. Because of the low natural abundance levels of ^{13}C (~1%), it is advantageous to carry out such experiments on highly enriched, uniformly labeled samples, especially since such samples are often available from structure determination studies. Moreover, the use of uniformly labeled samples allows the possibility of the measurement of the dynamics at every carbon site in the molecule using only a single sample.

Measurement of ^{13}C relaxation times in highly enriched, ^{13}C uniformly labeled molecules presents a number of significant challenges, however. The presence of large carbon-carbon scalar couplings can seriously limit the resolution in the ^{13}C dimension of spectra unless precautions are taken, and dipolar couplings between adjacent carbons can influence the measured carbon relaxation rates. The relative contribution to the relaxation of a ^{13}C nucleus from singly attached carbon and proton spins can be assessed in the macromolecular limit by including only the

® Abstract published in *Advance ACS Abstracts*, July 15, 1994.

(1) Kay, L. E.; Ikura, M.; Tschudin, R.; Bax, A. *J. Magn. Reson.* **1990**, *89*, 496.
(2) Ikura, M.; Kay, L. E.; Bax, A. *Biochemistry* **1990**, *29*, 4569.
(3) Clore, G. M.; Gronenborn, A. M. *Prog. Nucl. Magn. Reson. Spectrosc.* **1991**, *23*, 43.
(4) Bax, A.; Grzesiek, S. *Acc. Chem. Res.* **1993**, *26*, 131.
(5) Torchia, D. A.; Nicholson, L. K.; Cole, H. B. R.; Kay, L. E. Heteronuclear NMR Studies of the Molecular Dynamics of Staphylococcal Nuclease. In *Topics in Molecular and Structural Biology Series: NMR of Proteins*; Clore, G. M., Gronenborn, A. M., Eds.; The Macmillan Press Ltd.: Basingstoke, U.K., 1993.
(6) Peng, J.; Hyberts, S.; Wagner, G. Studies of Protein Dynamics by NMR. In *Topics in Molecular and Structural Biology Series: NMR of Proteins*; Clore, G. M., Gronenborn, A. M., Eds.; The Macmillan Press Ltd.: Basingstoke, U.K., 1993.
(7) Kay, L. E.; Torchia, D. A.; Bax, A. *Biochemistry* **1989**, *28*, 8972.
(8) Clore, G. M.; Driscoll, P. C.; Wingfield, P. T.; Gronenborn, A. M. *Biochemistry* **1990**, *29*, 7387.
(9) Kordel, J.; Skelton, N. J.; Akke, M.; Palmer, A. G.; Chazin, W. J. *Biochemistry* **1992**, *31*, 4856.
(10) Schneider, D. M.; Dellwo, M. J.; Wand, A. J. *Biochemistry* **1992**, *31*, 3645.
(11) Stone, M. J.; Fairbrother, W. J.; Palmer, A. G.; Reizer, J.; Saier, M. H.; Wright, P. E. *Biochemistry* **1992**, *31*, 4394.
(12) Peng, J.; Wagner, G. *Biochemistry* **1992**, *31*, 8571.
(13) Henry, G. D.; Weiner, J. H.; Sykes, B. D. *Biochemistry* **1986**, *25*, 590.
(14) Dellwo, M. J.; Wand, A. J. *J. Am. Chem. Soc.* **1989**, *111*, 4571.
(15) Palmer, A. G.; Rance, M.; Wright, P. E. *J. Am. Chem. Soc.* **1991**, *113*, 4371.
(16) Nicholson, L. K.; Kay, L. E.; Baldisseri, D. M.; Arango, J.; Young, P. E.; Bax, A.; Torchia, D. A. *Biochemistry* **1992**, *31*, 5253.
(17) Palmer, A. G.; Hochstrasser, R. A.; Millar, D. P.; Rance, M.; Wright, P. E. *J. Am. Chem. Soc.* **1993**, *115*, 6333.

0002-7863/94/1516-8266$04.50/0

relevant gyromagnetic ratios and distance factors involved and retaining only the dominant spectral density terms via the approximation

$$\rho_{HC}/\rho_{CC} = 3(\gamma_H^2/\gamma_C^2)(R_{CC}/R_{HC})^6(\omega_c\tau_c)^{-2} \quad (1)$$

where ρ_{HC} (ρ_{CC}) denotes the contribution to the selective relaxation rate of the ^{13}C nucleus from an attached ^1H (^{13}C), γ_j is the gyromagnetic ratio of spin j, R_{ij} is the distance between spins i and j, ω_c is the Larmor frequency for carbon, and τ_c is the overall tumbling time. Equation 1 predicts that the contribution to the ^{13}C relaxation rate from an adjacent carbon relative to the contribution from an adjacent proton grows as the square of the overall correlation time. As we discuss in detail later, contributions to the measurement of ^{13}C T_1 values from adjacent carbon spins are significant for macromolecules and must be included in the interpretation of the data in terms of motional models. An additional complication is the influence of carbon–carbon couplings on the measurement of T_2 and $T_{1\rho}$ values in uniformly labeled molecules. In the case of T_2 values determined using the well-known Carr–Purcell–Meiboom–Gill pulse scheme[18,19] (CPMG), the spin echo envelope can be modulated by the effects of ^{13}C–^{13}C couplings.[20a–c] In addition, during the CPMG relaxation time, magnetization can be transferred throughout a scalar coupled network (i.e., essentially throughout a complete amino acid), resulting in an effective averaging of measured T_2 values over all carbons involved in the transfer process. The measurement of $T_{1\rho}$ values can also be influenced by this Hartmann–Hahn transfer.[21]

With these problems in mind, we present a study which assesses the feasibility of the measurement of $^{13}C^{\alpha}$ relaxation properties in highly enriched (>95%), uniformly ^{13}C-labeled proteins. In order to carry out these "feasibility" experiments with very high signal-to-noise ratios, a sample consisting of approximately equimolar amounts of $^{13}C^{\alpha}$-alanine and $^{13}C_3$-alanine dissolved in perdeuterated glycerol was prepared. The steep viscosity dependence of glycerol with temperature allows measurement and comparison of $^{13}C^{\alpha}$ relaxation properties of singly and uniformly labeled molecules over a wide range of overall rotational correlation times, τ_c, including τ_c values on the order of 5–15 ns, typical for proteins of ~100–200 amino acids. The use of a single sample ensures that $^{13}C^{\alpha}$ measurements in singly and uniformly labeled molecules are performed under identical conditions. $^{13}C^{\alpha}$ T_1, $T_{1\rho}$, and ^1H–^{13}C steady-state NOE measurements at a number of different temperatures are presented, and differences in carbon relaxation properties in $^{13}C^{\alpha}$-alanine and $^{13}C_3$-alanine are rationalized through a consideration of the influence of the neighboring carbon spins. Pulse schemes for the measurement of relaxation properties of $^{13}C^{\alpha}$ nuclei in uniformly ^{13}C-labeled proteins are presented, followed by some results for $^{13}C^{\alpha}$ relaxation measurements on a uniformly ^{13}C,^{15}N-labeled recombinant C-terminal SH2 domain of phospholipase C-γ1 (105 amino acids) complexed with a 12 residue phosphopeptide from the platelet-derived growth factor receptor (PDGFR).

Experimental Section

98% uniform glycerol-d_8, 99% $^{13}C^{\alpha}$-alanine, and 99% $^{13}C_3$-alanine were purchased from Cambridge Isotope Laboratories. Approximately 3 mg each of $^{13}C^{\alpha}$-alanine and $^{13}C_3$-alanine were dissolved in 500 μL of glycerol. D_2O in an external capillary was used for the lock.

A 1.5 mM sample consisting of a uniformly ^{15}N,^{13}C-labeled recombinant fragment of the C-terminal SH2 domain of phospholipase C-γ1 (PLC-γ1) complexed with a 12 residue phosphopeptide from the PDGFR was prepared as described previously.[22a,b] The sample was dissolved in D_2O, 0.1 M sodium phosphate, pD 6.2, and experiments were performed at 30 °C.

All experiments were performed at 500/600 MHz on Varian UNITY spectrometers equipped with pulsed field gradient units and a triple resonance probe with an actively shielded z gradient. For each T_1 and $T_{1\rho}$ relaxation experiment, between 8 and 12 time points were recorded extending to approximately 1 × T_1 or 1 × $T_{1\rho}$ in the time domain. For example, in the case of T_1 and $T_{1\rho}$ data recorded for alanine dissolved in glycerol at 20 °C, values of T used were 48, 96, ..., 576 ms (T_1) and 4, 8, ..., 48 ms ($T_{1\rho}$). For the case of data recorded on the SH2 fragment complexed with the PDGFR peptide, experiments with delays of T = 5.1, 25.3, 55.6, 106.1, 156.6, 207.1, 277.9, 358.7, 439.5, and 520.4 ms (T_1 at 500 MHz), T = 5.1, 75.8, 156.7, 227.5, 308.4, 379.2, 460.1, 530.9, 611.8, and 682.6 ms (T_1 at 600 MHz), and T = 4.0, 12.1, 20.1, 28.1, 36.2, and 44.2 ms ($T_{1\rho}$ at 500 MHz) were recorded. All experiments recorded on alanine were repeated at least twice, and average values are reported. Relaxation data were fit to an equation of the form $y = A\exp(-t/T_i)$ $\{i = 1, 1\rho\}$ using least-squares techniques. Error estimates are based on Monte Carlo error analyses.[15,23]

Pulse Sequences Used To Measure $^{13}C^{\alpha}$ Relaxation Properties in Uniformly ^{13}C-Labeled Molecules

Figures 1a–c illustrate the pulse schemes used to record the $^{13}C^{\alpha}$ T_1 (1a) and $T_{1\rho}$ (1b) relaxation times as well as the ^1H–^{13}C steady-state NOE (1c) in highly enriched, uniformly ^{13}C,^{15}N-labeled proteins. For measurement of relaxation properties of $^{13}C^{\alpha}$-alanine in the alanine/glycerol sample, the intervals extending from points a to b in Figure 1 are replaced by the scheme indicated in Figure 1d. In the following we first discuss the differences in the sequences used to measure relaxation times in ^{13}C-alanine and ^{13}C-labeled proteins followed by a description of the common features of the sequences.

Separation of signals originating from $^{13}C^{\alpha}$ magnetization from either singly or uniformly ^{13}C-labeled alanine is achieved using difference spectroscopy in a manner similar to the approach exploited by Grzesiek and Bax to record $^{13}C^{\beta}$–$^1H^{\beta}$ correlation maps of aromatic residues.[24] Briefly, in the case of experiments to measure T_1 and $T_{1\rho}$ values, magnetization is transferred from ^1H to ^{13}C via an INEPT transfer,[25] and antiphase ^{13}C magnetization is allowed to refocus for an interval of $\tau_b = 0.5/J_{CH}$, where J_{CH} is the one-bond $^1H^{\alpha}$–$^{13}C^{\alpha}$ scalar coupling. Subsequently, ^1H decoupling is employed to ensure that carbon magnetization remains in phase with respect to ^1H–^{13}C couplings for the remainder of the duration $2\delta'$. During the period $2\delta' = 1/(J_{c\alpha c'})$, where $J_{c\alpha c'}$ is the $^{13}C^{\alpha}$–$^{13}C'$ (C' = carbonyl) coupling constant, $^{13}C^{\alpha}$ evolution due to the $J_{c\alpha c'}$ coupling is refocused in scheme 1 of Figure 1d (i.e., where $^{13}C'$ 180° pulses are applied at positions a' and b'), while carbon magnetization evolves due to this coupling in scheme 2 (where $^{13}C'$ 180° pulses are applied at positions a' and c'). For the population of molecules which are uniformly carbon-labeled, evolution of $^{13}C^{\alpha}$ magnetization due to the $^{13}C^{\alpha}$–$^{13}C^{\beta}$ scalar coupling would normally proceed for the duration $2\delta'$ as well, resulting in a significant decrease in the intensity of the observed signal. In order to refocus the effects of the one-bond $^{13}C^{\alpha}$–$^{13}C^{\beta}$ couplings, a $90_{\phi2}$-ξ-$90_{\phi2}$ element[26] is inserted in the center of the $2\delta'$ period, with $\xi = 0.5/\Delta_{\alpha,\beta} - (4/\pi)\tau_{90}$, where $\Delta_{\alpha,\beta}$ is the chemical shift difference between $^{13}C^{\alpha}$ and $^{13}C^{\beta}$ carbons (in Hz) and τ_{90} is the $^{13}C^{\alpha}$ $90_{\phi2}$ pulse width. (The carbon pulses are applied on resonance for the $^{13}C^{\alpha}$ spin.) The $(4/\pi)\tau_{90}$ term compensates for the evolution of magnetization which occurs during the application of the $90_{\phi2}$ pulses.[27,28] Note

(18) Carr, H. Y.; Purcell, E. M. *Phys. Rev.* **1954**, *94*, 630.
(19) Meiboom, S.; Gill, D. *Rev. Sci. Instrum.* **1958**, *29*, 688.
(20) (a) Wells, E. J.; Gutowsky, H. S. *J. Chem. Phys.* **1965**, *43*, 3414. (b) Allerhand, A. *J. Chem. Phys.* **1966**, *44*, 1. (c) Freeman, R.; Hill, H. D. W. *Dynamic Nuclear Magnetic Resonance Spectroscopy*; Jackman, L. M., Cotton, F. A., Eds.; Academic Press: San Diego, CA, 1975.
(21) Hartmann, S. R.; Hahn, E. L. *Phys. Rev.* **1962**, *128*, 2042.
(22) (a) Farrow, N. A.; Muhandiram, D. R.; Singer, A. U.; Pascal, S. M.; Kay, C. M.; Gish, G.; Shoelson, S. E.; Pawson, T.; Forman-Kay, J. D.; Kay, L. E. *Biochemistry* **1994**, *33*, 5984–6003. (b) Pascal, S. M.; Singer, A. U.; Gish, G.; Yamazaki, T.; Shoelson, S. E.; Pawson, T.; Kay, L. E.; Forman-Kay, J. D. *Cell* **1994**, *77*, 461–472.
(23) Kamath, U.; Shriver, J. W. *J. Biol. Chem.* **1989**, *264*, 5586.
(24) Grzesiek, S.; Bax, A. *J. Biomol. NMR* **1993**, *3*, 185.
(25) Morris, G. A.; Freeman, R. *J. Am. Chem. Soc.* **1979**, *101*, 760.
(26) Yamazaki, T.; Forman-Kay, J. D.; Kay, L. E. *J. Am. Chem. Soc.* **1993**, *115*, 11054.

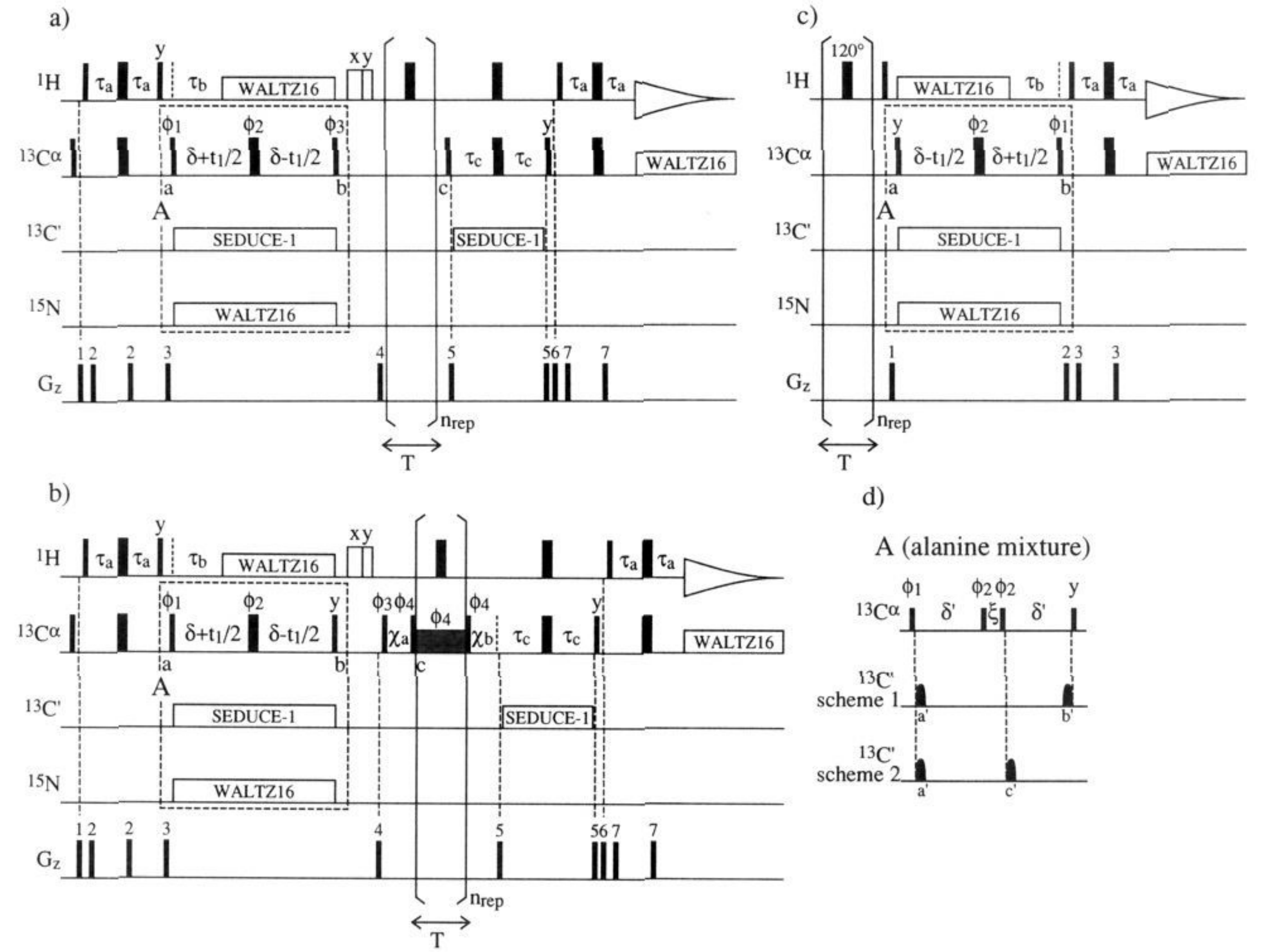

Figure 1. Pulse sequences for the measurement of $^{13}C^{\alpha}$ T_1 (a), $T_{1\rho}$ (b), and steady-state ^1H–^{13}C NOE values (c) in highly enriched, uniformly ^{15}N,^{13}C-labeled protein samples. The region in the sequences enclosed by the box (dashed lines) marked A in Figures 1a–c is to be replaced by A in Figure 1d for measuring relaxation properties in the alanine system considered in the text. Narrow (wide) pulses correspond to a flip angle of 90° (180°). Unless indicated otherwise, the pulses are applied along the x axis. All proton pulses are applied with a 24-kHz field, with the exception of the 120° pulses employed for ^1H saturation in Figure 1c, where a field of ~12 kHz was employed. ^1H WALTZ[61] decoupling was achieved using a 6.6-kHz field. All carbon pulses (centered at 58 ppm) in Figures 1a–c are applied using an 18-kHz field with WALTZ[61] decoupling during acquisition achieved using a 1.8-kHz field. In the case of Figure 1d, the $^{13}C^{\alpha}$ pulses (53 ppm) are applied using a 4.0-kHz field so as not to perturb carbonyl spins. The 180° carbonyl pulses are applied using the shape profile of a SEDUCE-1[62] element in an off-resonance manner using phase-modulated[63,64] pulses of duration 250 μs. Note that C′ pulses are applied on opposite sides of the $90_{\phi2}$-ξ-$90_{\phi2}$ element to compensate for Bloch–Siegert shifts that only a single C′ pulse would generate.[24,30] SEDUCE-1[62] carbonyl decoupling during the constant time evolution delay, 2δ, is achieved using a field centered at 175 ppm (350-μs 90° SEDUCE pulses; 1.6-kHz field at peak height), while ^{15}N decoupling is employed using a 1-kHz WALTZ[61] field centered at 119 ppm. Immediately after point b in the sequences of Figures 1a and b purge pulses of durations of 1.5 and 0.9 ms (10 kHz) can be applied along the x and y axes, respectively, to eliminate any residual water which would interfere with quantitation of cross peak intensities. The delays used are as follows: τ_a = 1.7 ms; τ_b = 3.57 ms; τ_c = 1.55 ms; δ = 13.3 ms $\{1/(2J_{cc})\}$; and δ' = 9.1 ms $\{1/(2J_{c\alpha c'})\}$. The delay χ_a is set according to the relation $\chi_a = 1/(2\pi\nu_1) - (4/\pi)\tau_{90}$, where ν_1 is the strength (in Hz) of the spin lock field employed and τ_{90} is set equal to the $90°_{\phi3(\phi4)}$ ^{13}C pulse width. The delay χ_b is set to $\chi_b = 1/(2\pi\nu_1)$. A field strength of 2.2 kHz (~114-μs 90° pulse) was employed in the $T_{1\rho}$ measurements. The delay ξ (Figure 1d) is set according to the relation $\xi = 0.5/\Delta_{\alpha,\beta} - (4/\pi)\tau_{90}$, where $\Delta_{\alpha,\beta}$ is the chemical shift difference between $^{13}C^{\alpha}$ and $^{13}C^{\beta}$ carbons and τ_{90} is the $^{13}C^{\alpha}$ $90_{\phi2}$ pulse length (see text). For measuring relaxation properties in the alanine/glycerol system, the $^{13}C^{\alpha}$ $90_{\phi2}$ pulse width is set to $\sqrt{15}/(4\,\Delta_{\alpha,c'})$, where $\Delta_{\alpha,c'}$ is the chemical shift difference between $^{13}C^{\alpha}$ and $^{13}C'$ spins so as not to perturb carbonyl magnetization.[1] In Figure 1a, ^1H 180° pulses are applied every 5 ms during the T delay to eliminate the effects of cross correlation between ^1H–^{13}C dipolar interactions and ^{13}C CSA[52] or cross correlation effects between ^{13}C–^{13}C and ^1H–^{13}C dipolar interactions, while in the sequence of Figure 1b, ^1H 180° pulses are applied every 4 ms.[53,54] The phase cycling employed is as follows. Figure 1a: $\phi1 = x$; $\phi2 = (x,y,-x,-y)$; $\phi3 = 4(y), 4(-y)$; rec = $2(x,-x), 2(-x,x)$. Figure 1b: $\phi1 = x$; $\phi2 = (x,y,-x,-y)$; $\phi3 = 4(y), 4(-y)$; $\phi4 = 8(x), 8(-x)$; rec = $2(x,-x), 2(-x,x)$. Figure 1c: $\phi1 = x$; $\phi2 = (x,y,-x,-y)$; rec = $(x,-x)$. For sequences a and b, the gradients employed are $g1$ = (0.5 ms, 5 G/cm), $g2$ = (0.3 ms, 3 G/cm), $g3$ = (1.0 ms, 8 G/cm), $g4$ = (0.5 ms, 10 G/cm), $g5$ = (0.1 ms, 4 G/cm), $g6$ = (0.5 ms, 5 G/cm), and $g7$ = (0.4 ms, 2 G/cm), while for sequence c, $g1$ = (0.5 ms, 15 G/cm), $g2$ = (0.5 ms, 10 G/cm), and $g3$ = (0.4 ms, 2 G/cm). For protein applications, two-dimensional data sets are recorded with quadrature in F_1 obtained by incrementing the phase $\phi1$ using States-TPPI.[65] In the absence of gradients, the $^{13}C^{\alpha}$ 90° pulse at the outset of the sequences of Figures 1a and b should be removed, and the ^1H 90° pulse immediately preceeding the final $2\tau_a$ period in each of the sequences should be phase cycled $8(x), 8(-x)$ (T_1); $16(x), 16(-x)$ (T_2); or $4(x), 4(-x)$ (NOE) and the receiver phase inverted. A homospoil pulse should be employed in lieu of the gradient pulse $g4$ in Figures 1a and b.

that these $90_{\phi2}$ pulses must be adjusted in duration to $\sqrt{15}/(4\Delta_{\alpha,c'})$, where $\Delta_{\alpha,c'}$ is the chemical shift difference (in Hz) between $^{13}C^{\alpha}$ and $^{13}C'$ spins, so as not to perturb carbonyl magnetization.[1] At points b′ in each of the sequences, the $^{13}C^{\alpha}$ magnetization from the uniformly ^{13}C-labeled alanine molecules

(27) Ernst, R. R.; Bodenhausen, G.; Wokaun, A. *Principles of Nuclear Magnetic Resonance in One and Two Dimensions*; Clarendon Press: Oxford, U.K., 1987.

(28) Marion, D.; Bax, A. *J. Magn. Reson.* **1988**, *78*, 186.

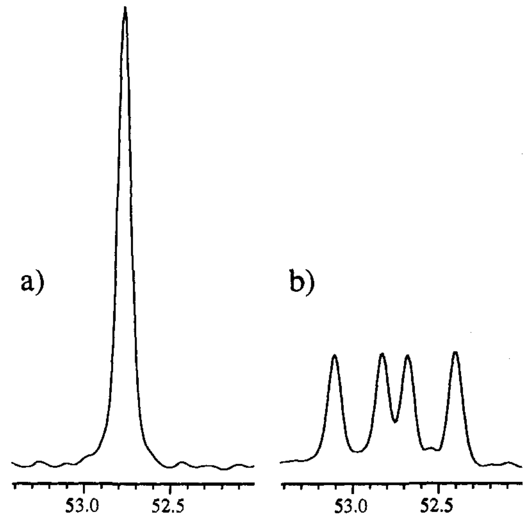

Figure 2. Carbon spectra showing the ${}^{13}C^{\alpha}$ region of singly labeled (a) and uniformly labeled (b) alanine dissolved in perdeuterated glycerol. The sample used consists of an equimolar mixture of ${}^{13}C^{\alpha}$-alanine and ${}^{13}C_3$-alanine. The pulse sequence used to separate the signals from singly and uniformly carbon-labeled molecules is essentially that of Figure 1d, with the exception that ${}^1H$ decoupling is employed throughout the $2\delta'$ period and during acquisition and the final ${}^{13}C^{\alpha}$ $90°_y$ pulse is omitted (i.e., magnetization acquired immediately after the second δ' delay). The resultant spectra are generated as either the sum or the difference of signals obtained with the carbonyl pulses positioned as in either scheme 1 or scheme 2 of Figure 1d.

is given by Mo′ and Mo′ $\cos(2\pi J_{c\alpha c'}\delta')$ for schemes 1 and 2, respectively, while ${}^{13}C^{\alpha}$ magnetization from the singly labeled population of alanine molecules in the sample is given by Mo for both schemes 1 and 2 (i.e., identical results obtained in both cases). By tuning $2\delta' = 1/(J_{c\alpha c'})$, the sum of the signals obtained in schemes 1 and 2 gives a ${}^{13}C^{\alpha}$ spectrum originating from the singly labeled ${}^{13}C$ population of molecules, while the difference gives the spectrum of the uniformly labeled alanine, as illustrated in Figure 2.

In the case of the NOE experiment, magnetization must originate on carbon, and ${}^1H$ decoupling begins immediately after excitation of carbon magnetization. Decoupling is terminated $\tau_b = 1/(2J_{HC})$ prior to the INEPT transfer back to protons for observation. An identical strategy to that used in the T_1 and $T_{1\rho}$ measurements for the separation of uniformly and singly labeled alanine molecules is employed in this case.

For protein applications, the need for adequate resolution dictates that two-dimensional ${}^1H$–${}^{13}C$ correlation spectra be recorded. In this case, a constant time period to record the evolution of carbon magnetization must be employed.[29,30] The use of constant time spectroscopy with a constant time delay $2\delta = 1/J_{CC}$, where J_{CC} is the (uniform) aliphatic carbon–carbon coupling constant, ensures that despite the fact that highly enriched, uniformly ${}^{13}C$-labeled proteins are employed in the measurements, the presence of ${}^{13}C$–${}^{13}C$ couplings does not degrade resolution in the spectra. Because carbonyl decoupling is employed for the complete constant time duration, the 180° ${}^{13}C$ pulse of phase $\phi 2$ can be applied with high power in this case.

After the intervals 2δ (protein applications) or $2\delta'$ (alanine sample) in each of the pulse sequences, the course of evolution of magnetization varies depending on whether T_1, $T_{1\rho}$, or NOE measurements are made. At point b in the sequence of Figure 1a, ${}^{13}C$ magnetization is returned to the z axis by the $90_{\phi 3}$ ${}^{13}C$ pulse immediately preceding b, and residual H_2O, which would interfere with observation of ${}^{13}C^{\alpha}$–${}^1H^{\alpha}$ cross peaks, is eliminated through the application of scrambling pulses and a gradient. Subsequently, longitudinal relaxation proceeds for a time T, after which magnetization is transferred back to ${}^1H$ for observation. In the sequence used to measure $T_{1\rho}$ (Figure 1b), the magnetization is returned to the z-axis following the 2δ period at point b, and residual H_2O is eliminated as in the sequence of Figure 1a. The $90_{\phi 3}$-χ_a-$90_{\phi 4}$ scheme that follows eliminates the offset dependence which would normally accompany the projection of transverse carbon magnetization onto the effective field generated by the combination of the spin lock field of strength ν_1 (Hz) and applied with phase $\phi 4$ and the residual Zeeman field.[31] The value of χ_a is adjusted according to $\chi_a = 1/(2\pi\nu_1) - (4/\pi)\tau_{90}$, with τ_{90} set equal to the $90°_{\phi 3(\phi 4)}$ ${}^{13}C$ pulse width. Note that the $(4/\pi)\tau_{90}$ term compensates for the chemical shift evolution which occurs during application of the two 90° pulses surrounding the χ_a delay. Consider a spin j at offset Δ_j (Hz) from the carrier. If $\phi 3 = y$ and $\phi 4 = x$, then at point c in the sequence of Figure 1b, the magnetization is given by

$$C_x^j \cos(2\pi\Delta_j\chi') + C_z^j \sin(2\pi\Delta_j\chi') \tag{2}$$

where $\chi' = 1/(2\pi\nu_1)$ and C_x^j, C_z^j are the x and z components of magnetization, respectively, of spin j. Thus, the magnetization associated with each spin j resides in the x–z plane and makes an angle (radians) of $2\pi\Delta_j\chi' = \Delta_j/\nu_1$ with respect to the x axis. Similarly, the effective field experienced by spin j during application of a spin lock pulse along the x axis and of duration T makes an angle of

$$\theta = \arctan(\Delta_j/\nu_1) \tag{3}$$

with respect to the x axis. For the case of spin lock fields on the order of ~2 kHz and assuming that the carbon carrier is positioned in the center of the ${}^{13}C^{\alpha}$ region so that $|\Delta_j| < 1.0$ kHz, eq 3 can be approximated as

$$\theta \sim (\Delta_j/\nu_1) \tag{4}$$

Thus both the effective field for spin j and the magnetization of spin j are collinear at the time of application of the spin lock field (point c in the sequence of Figure 1b). In contrast, if the $90_{\phi 3}$-χ_a-$90_{\phi 4}$ scheme were replaced by a single 90° pulse prior to the application of the spin lock field, then the component of the magnetization perpendicular to the spin lock field would decay in rapid order due to radiofrequency (rf) inhomogeneity and only the projection of the magnetization onto the spin lock field would remain. In this case, the fraction $1 - \cos(\theta)$ of the original magnetization would be lost due to rf inhomogeneity effects. At the conclusion of the spin lock pulse, spin locked magnetization is restored to the x–y plane via a $90_{\phi 4}$ pulse followed by a delay $\chi_b = 1/(2\pi\nu_1)$. (Note that the pulse width of the second $90_{\phi 4}$ pulse is compensated for by the width of the subsequent ${}^{13}C^{\alpha}$ $90y$ pulse.) Magnetization is subsequently transferred back to protons for observation. If carbon magnetization were transferred back to protons via a reverse INEPT immediately following the spin lock pulse, then an additional $1 - \cos(\theta)$ of the signal would be lost. Griesinger and Ernst have employed a similar strategy for the improvement of signal-to-noise ratios in ROESY spectra by elimination of the offset dependence of cross peak amplitudes.[31]

${}^1H$–${}^{13}C$ steady-state NOE values are obtained by recording two spectra, one with and one without the NOE effect,[7] as indicated in Figure 1c. As is the case in the previous experiments, for protein applications, ${}^{13}C$ chemical shift is recorded in a constant time manner, and the magnetization is subsequently transferred to protons for observation via a reverse INEPT scheme.

(29) Santoro, J.; King, G. C. *J. Magn. Reson.* **1992**, *97*, 202.
(30) Vuister, G. W.; Bax, A. *J. Magn. Reson.* **1992**, *98*, 428.
(31) Griesinger, C.; Ernst, R. R. *J. Magn. Reson.* **1987**, *75*, 261.

Table 1. $^{13}C^\alpha$ T_1 Values (ms) Measured for Singly (T_1^s) and Uniformly (T_1^u) ^{13}C-Labeled Alanine Dissolved in Perdeuterated Glycerol

Temp (°C)	τ_c[a]	T_1^s	T_1^u[b]	$\{1/T_1^u - 1/T_1^s\}$[c]	$\{1/T_1^u - 1/T_1^s\}_{calc}$[d]
40	1.0	275.4 ± 1.4	262.6 ± 1.6 (4.6%)	0.18	0.16
30	2.4	351.9 ± 0.8	331.1 ± 1.3 (5.9%)	0.18	0.17
20	6.1	581.6 ± 1.5	503.3 ± 1.7 (13.5%)	0.27	0.26
10	16.7	1070 ± 9	642 ± 5 (40%)	0.62	0.60

[a] Approximate correlation times (ns) estimated from the $T_{1\rho}^s$ values assuming isotropic motion. [b] In parentheses is shown the percent difference in T_1^u and T_1^s values ($\{T_1^s - T_1^u\}/T_1^s$). [c] Difference in experimental relaxation rates of the $^{13}C^\alpha$ spin in uniformly and singly labeled alanine. [d] Difference in relaxation rates of the $^{13}C^\alpha$ spin in uniformly and singly labeled alanine calculated using eq 6.

In all of the sequences, pulsed field gradients are employed to aid in the suppression of artifacts and in the elimination of signal from residual H_2O. In the case of sequences for the measurement of T_1 and $T_{1\rho}$ times, ^{13}C magnetization present at the outset of the experiment is effectively scrambled through the application of a carbon pulse followed by a pulsed field gradient.[32] Gradients can be applied on opposite sides of 180° pulses to ensure that only transverse magnetization present before the application of the 180° pulse is retained after its application.[33] In addition, gradients are employed during periods in which the desired magnetization is of the form I_zC_z, where I_z and C_z are the z components of ^{1}H and ^{13}C magnetization, respectively.[33] Although the desired magnetization is not affected by the application of gradients during this time, any transverse magnetization, which could give rise to potential artifacts in spectra, is eliminated by the application of a gradient pulse.

Results and Discussion

(i) Measurement of $^{13}C^\alpha$ T_1 Values. Table 1 shows $^{13}C^\alpha$ selective T_1 values measured at four different temperatures for uniformly (T_1^u) and singly (T_1^s) labeled alanine molecules. The overall rotational correlation times, τ_c, are calculated on the basis of the $T_{1\rho}^s$ values assuming molecules of spherical symmetry. It is readily apparent that, while similar T_1 values are obtained at 40 °C, where the correlation time is the smallest, as the τ_c value increases, the discrepancy between T_1^s and T_1^u values becomes significant. Clearly, for slowly tumbling molecules, the effects of the adjacent ^{13}C spins on the longitudinal relaxation of the $^{13}C^\alpha$ spin are not negligible. The longitudinal relaxation of the $^{13}C^\alpha$ spin during time T for the uniformly ^{13}C-labeled alanine case is governed by the relaxation equation[34]

$$d/dT\, C_z^\alpha = -\rho^u_{c\alpha}(C_z^\alpha - C_z^{\alpha,0}) - \sigma_{c\alpha,c\beta}(C_z^\beta - C_z^{\beta,0}) - \sigma_{c\alpha,c'}(C_z' - C_z'^{,0}) - \sigma_{c\alpha,H\alpha}(I_z^\alpha - I_z^{\alpha,0}) \quad (5)$$

where C_z^α, C_z^β, and C_z' are the carbon α, β, and carbonyl longitudinal magnetizations, respectively, $C_z^{i,0}$ is the equilibrium longitudinal magnetization of spin i, I_z^α is the H$^\alpha$ proton magnetization, and the autorelaxation and cross relaxation rates are given by ρ and σ terms, respectively. It is easy to show that the measured relaxation time course of C_z^α depends not only on the values of ρ and σ but also on the initial states of longitudinal magnetization of all spins dipolar coupled to the $^{13}C^\alpha$ nucleus. Similar equations pertain for the other carbon and proton spins that are dipolar coupled to the $^{13}C^\alpha$ spin. In the general case, $\rho^u_{c\alpha}$ includes contributions from all dipolar coupled spins. For the case of uniformly ^{13}C-labeled alanine, the H$^\alpha$, C$^\beta$, and C$'$ spins contribute to the relaxation of the $^{13}C^\alpha$ nucleus, and

$$\rho^u_{c\alpha} = \rho_{c\alpha,H\alpha} + \rho_{c\alpha,c\beta} + \rho_{c\alpha,c'} + \rho_0 \quad (6.1)$$

where $\rho_{c\alpha,i}$ is given by[35]

$$0.1\gamma_C^2\gamma_i^2h^2/(4\pi^2r^6)[3J(\omega_C) + J(\omega_C - \omega_i) + 6J(\omega_C + \omega_i)] \quad (6.2)$$

and $\sigma_{c\alpha,i}$ is given by[35]

$$0.1\gamma_C^2\gamma_i^2h^2/(4\pi^2r^6)[6J(\omega_C + \omega_i) - J(\omega_C - \omega_i)] \quad (6.3)$$

and ρ_0 includes contributions from all other relaxation mechanisms such as ^{13}C chemical shift anisotropy, the ^{15}N–^{13}C dipolar interaction for the case of ^{15}N-labeled molecules, or ^{14}N–^{13}C dipolar and scalar relaxation of the second kind contributions for the case where ^{15}N labeling is not employed. The effects of cross correlation have been neglected in eqs 5 and 6. We will return to this point later on. In eq 6, γ_i is the gyromagnetic ratio of spin i, h is Planck's constant, r is the distance between spins C$^\alpha$ and i, and $J(\omega)$ is a spectral density function defined as $J(\omega) = \tau_c/[1 + (\omega\tau_c)^2]$ in the case of uniform rotational diffusion with a correlation time τ_c. In contrast, only the first and last terms of eq 6.1 apply for alanine molecules, which are labeled only in the C$^\alpha$ position; that is, $\rho^s_{c\alpha} = \rho_{c\alpha,H\alpha} + \rho_0$. It is particularly important to recognize that for $\rho_{c\alpha,i}$, where i is a carbon spin, the second term of eq 6.2 is proportional to $J(0)$. Note that $J(0)$ spectral density terms increase with increasing τ_c, while $J(\omega)$ terms ($\omega \neq 0$) decrease. In applications involving macromolecules, such terms are significant. Table 1 shows that the differences in experimentally measured relaxation rates ($\rho^u_{c\alpha}-\rho^s_{c\alpha}$) can be accounted for by including the additional sources of relaxation due to the neighboring carbon spins (eq 6) in the uniformly ^{13}C-labeled sample.

As will be described in detail below, provided that the decay of magnetization is sampled for values of T such that $T < \sim 1/\rho^u_{c\alpha}$, the sequence of Figure 1a provides an accurate measure of $\rho^u_{c\alpha}$ for uniformly ^{13}C-labeled molecules. For molecules labeled only in the $^{13}C^\alpha$ position, accurate values of $\rho^s_{c\alpha}$ can be obtained even for T values greater than $1/\rho^s_{c\alpha}$, since in this case cross relaxation with adjacent carbons cannot occur. Note that proton saturation is carried out during the relaxation time T for measurement of both $\rho^u_{c\alpha}$ and $\rho^s_{c\alpha}$.

Figure 3 illustrates the autorelaxation rates for the $^{13}C^\alpha$ carbon for singly labeled ($\rho^s_{c\alpha}$) and uniformly labeled ($\rho^u_{c\alpha}$) alanine assuming isotropic motion. It is clear that while $\rho^s_{c\alpha} \sim \rho^u_{c\alpha}$ for small values of τ_c ($\tau_c < 1$ ns), the difference becomes significant in the case of macromolecules. Note that as τ_c increases, the contributions to $\rho^u_{c\alpha}$ from $\rho_{c\alpha,c\beta}$ and $\rho_{c\alpha,c'}$ increase relative to $\rho_{c\alpha,H\alpha}$ since the former terms contain expressions proportional to $J(0)$, while $\rho_{c\alpha,H\alpha}$ does not. Thus, despite the fact that $\gamma_C^2\gamma_H^2h^2/(4\pi^2r_{HC}^6) \gg \gamma_C^2\gamma_C^2h^2/(4\pi^2r_{CC}^6)$, the results presented in Table 1 and Figure 3 illustrate that the contributions to the measured ^{13}C relaxation times from adjacent carbons cannot be neglected. The upper panel in Figure 3 shows the cross relaxation rate between a $^{13}C^\alpha$ spin and a one-bond coupled carbon spin separated by an internuclear distance of 1.53 Å[36] as well as the cross relaxation rate between an $^1H^\alpha$–$^{13}C^\alpha$ pair separated by 1.10 Å. Note the change in sign of $\sigma_{c\alpha,H\alpha}$ relative to the homonuclear cross relaxation term.

Inspection of the phase cycle of the sequence of Figure 1a shows that the ^{13}C 90° pulse of phase $\phi 3$ places carbon magnetization along the $+z$ and $-z$ axes on alternate scans. As Sklenar et al.[37] have discussed previously, this ensures that the relaxation rate does not depend on the equilibrium values of longitudinal magnetization, C_z^i. Denoting the z component of $^{13}C^i$ magnetization by $C_z^i(T,\uparrow)$, or $C_z^i(T,\downarrow)$ depending on whether

(32) Kay, L. E. *J. Am. Chem. Soc.* **1993**, *115*, 2055.
(33) Bax, A.; Pochapsky, S. *J. Magn. Reson.* **1992**, *99*, 638.
(34) Noggle, J. H.; Schirmer, R. E. *The Nuclear Overhauser Effect*; Academic Press: New York, 1971.
(35) Abragam, A. *The Principles of Nuclear Magnetism*; Oxford University Press: Oxford, U.K., 1961.
(36) Fawcett, J. K.; Camerman, N.; Camermon, A. *Acta Crystallogr.* **1975**, *B31*, 658.
(37) Sklenar, V.; Torchia, D. A.; Bax, A. *J. Magn. Reson.* **1987**, *73*, 375.

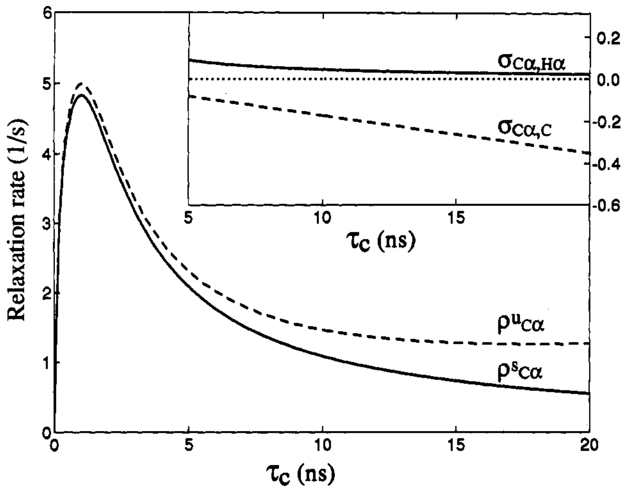

Figure 3. Relaxation rates as a function of isotropic correlation time, τ_c. Values of $^{13}C^\alpha$ autorelaxation rates in uniformly ($\rho^u_{c\alpha}$) or singly labeled molecules ($\rho^s_{c\alpha}$) are indicated. Calculations assume that the dominant contributions to the relaxation of a C$^\alpha$ spin come from the dipolar coupling to a single ^{1}H spin as well as carbonyl and C$^\beta$ spins. The upper panel shows $^1H^\alpha$–$^{13}C^\alpha$ and $^{13}C^\alpha$–$^{13}C^\beta$ or $^{13}C^\alpha$–$^{13}C'$ cross relaxation rates plotted as a function of correlation time. Internuclear distances of 1.10 ($^1H^\alpha$–$^{13}C^\alpha$)[50] and 1.53 Å (^{13}C–^{13}C)[36] are assumed.

the initial state of the $^{13}C^\alpha$ magnetization at $T = 0$ is along the $+z$ or the $-z$ axis, respectively, we can write

$$d/dT\{\Delta C_z^\alpha(T)\} = -\rho^u_{c\alpha}\{\Delta C_z^\alpha(T)\} - \sigma_{c\alpha,c\beta}\{\Delta C_z^\beta(T)\} - \sigma_{c\alpha,c'}\{\Delta C_z'(T)\} - \sigma_{c\alpha,H\alpha}\{\Delta I_z^\alpha(T)\} \quad (7)$$

where $\Delta C_z^i(T) = C_z^i(T,\uparrow) - C_z^i(T,\downarrow)$ ($i = \alpha, \beta, '$) and $\Delta I_z^\alpha(T) = I_z^\alpha(T,\uparrow) - I_z^\alpha(T,\downarrow)$. In eq 7, the term proportional to $\sigma_{c\alpha,H\alpha}$ disappears since proton saturation occurs during the T delay, and hence $I_z^\alpha = 0$. Further simplification of eq 7 is possible by considering only the initial evolution of ΔC_z^α (i.e., small T values). The initial slope of the decay of $\Delta C_z^\alpha(T)$ is given by

$$d/dT\{\Delta C_z^\alpha(T)\}|_{T=0} = -\{\rho^u_{c\alpha} + \lambda^\beta\sigma_{c\alpha,c\beta} + \lambda'\sigma_{c\alpha,c'}\}\Delta C_z^\alpha(0) \quad (8.1)$$

where $\lambda^\beta = \Delta C_z^\beta(0)/\Delta C_z^\alpha(0)$ and $\lambda' = \Delta C_z'(0)/\Delta C_z^\alpha(0)$.

Equation 8.1 can be simplified by noting that before the INEPT transfer from $^1H \rightarrow {}^{13}C$, carbon magnetization is eliminated through the application of a ^{13}C 90° pulse followed by a gradient. Thus $C_z'(0,\uparrow) = C_z'(0,\downarrow) = 0$. We can therefore rewrite eq 8.1 as

$$d/dT\{\Delta C_z^\alpha(T)\}|_{T=0} = -\{\rho^u_{c\alpha} + \lambda^\beta\sigma_{c\alpha,c\beta}\}\Delta C_z^\alpha(0) \quad (8.2)$$

The initial rate of decay of the difference, $\Delta C_z^\alpha(T) = C_z^\alpha(T,\uparrow) - C_z^\alpha(T,\downarrow)$, depends, therefore, on the initial values of both $^{13}C^\alpha$ and $^{13}C^\beta$ z magnetization as well as the autorelaxation rate, $\rho^u_{c\alpha}$, and the cross relaxation rate, $\sigma_{c\alpha,c\beta}$, between the $^{13}C^\alpha$ and $^{13}C^\beta$ spins. The terms $\Delta C_z^\alpha(0)$ and $\Delta C_z^\beta(0)$ can be evaluated by considering a product operator description[27,38–40] of the sequence of Figure 1. We first focus our attention on the sequence used to measure $^{13}C^\alpha$ longitudinal relaxation in uniformly and singly labeled alanine molecules.

The relaxation times indicated in Table 1 for alanine dissolved in glycerol were measured from one-dimensional spectra obtained using the pulse sequence of Figure 1a with the regions from a to b substituted by the scheme in Figure 1d. In these experiments, the carbon carrier was positioned at the chemical shift of the $^{13}C^\alpha$ resonance. The $90_{\phi2}$-ξ-$90_{\phi2}$ sequence during the constant time period, $2\delta'$, ensures that evolution of the $^{13}C^\alpha$ magnetization due to both the effects of chemical shift as well as one-bond $^{13}C^\alpha$–$^{13}C^\beta$ scalar coupling is refocused at the end of the constant time period. In contrast, the careful adjustment of $\xi = 0.5/\Delta_{\alpha,\beta} - (4/\pi)\tau_{90}$ (where $\Delta_{\alpha,\beta}$ is the chemical shift difference (Hz) between $^{13}C^\alpha$ and $^{13}C^\beta$ carbons and τ_{90} is the $^{13}C^\alpha$ $90_{\phi2}$ pulse length) ensures that $^{13}C^\beta$ chemical shift evolution proceeds for the complete constant time period. It should be noted that incrementation of $\phi2$ by 90° inverts the phase of $\Delta C_z^\alpha(0)$, while the phase of $\Delta C_z^\beta(0)$ is unaffected. Since the phase of the receiver is inverted each time $\phi2$ is incremented by 90°, the net result is that, averaged over a complete phase cycle, the initial rate (i.e., $d/dT\{\Delta C_z^\alpha(T)\}|_{T=0}$) is proportional to $\rho^u_{c\alpha}$ alone. However, it is also the case that on a per scan basis the contribution of the second term of eq 8.2 to the initial rate of decay is very small. This is especially the case since the delay τ_b is adjusted to maximize transfer from proton magnetization to in-phase carbon magnetization for CH spin systems, and hence the transfer functions for CH_2 and CH_3 spin systems are inefficient. In order to evaluate this contribution, the values of $\Delta C_z^\alpha(0)$ and $\Delta C_z^\beta(0)$ are calculated for the case of the uniformly ^{13}C-labeled alanine to be

$$\Delta C_z^\alpha(0) = A\sin(2\pi J_{H\alpha C\alpha}\tau_a)\sin(\pi J_{H\alpha C\alpha}\tau_b)\exp(-2\delta'/T_{2,C\alpha})$$

$$\Delta C_z^\beta(0) = 3A'\sin(2\pi J_{H\beta C\beta}\tau_a)\sin(\pi J_{H\beta C\beta}\tau_b) \times \cos^2(\pi J_{H\beta C\beta}\tau_b)\exp(-2\delta'/T_{2,C\beta})\cos(2\pi\Delta_{\alpha,\beta}2\delta') \quad (9)$$

where J_{HiCi} is the one-bond coupling between H_i and C_i, $T_{2,Ci}$ is the transverse relaxation time of C_i, $2\delta' = 1/J_{c\alpha c'}$, and A and A' are factors which depend, among other things, on the delay between scans and the T_1 relaxation times of the H$^\alpha$ and H$^\beta$ spins, respectively. Neglecting relaxation, the quantity $[\Delta C_z^\beta(0)]/[\Delta C_z^\alpha(0)]$ is less than 0.08 for the case of alanine. Moreover, for correlation times less than ~15 ns, $|\sigma_{c\alpha,c\beta}/\rho^u_{c\alpha}| < 0.25$, and the second term of eq 8.2 makes a contribution of less than 2% to the measured initial rate of relaxation of C_z^α in a given scan (i.e., in the absence of phase cycling $\phi2$). Note that for isotropic motion and assuming equal C$^\alpha$–C$^\beta$ and C$^\alpha$–C$'$ internuclear distances,[36] $|\sigma_{c\alpha,c\beta}/\rho^u_{c\alpha}|$ increases to a maximum value of 0.5 in the limit of $\tau_c \rightarrow \infty$.

To this point our discussion has focused on the initial rate of change of $\Delta C_z^\alpha(T)$. In practice, it is of course not possible to measure the initial rate of decay with sufficient accuracy to ensure that the measured relaxation rate contains contributions from $\rho^u_{c\alpha}$ only (i.e., $\Delta C_z^\alpha(T) \propto \exp(-\rho^u_{c\alpha}T)$). In order to calculate the evolution of $\Delta C_z^\alpha(T)$ for times longer than the initial decay of magnetization, we consider, for the case of alanine, the system of equations

$$\frac{d}{dT}\begin{pmatrix}\{\Delta C_z^\alpha(T)\}\\ \{\Delta C_z^\beta(T)\}\\ \{\Delta C_z'(T)\}\end{pmatrix} = -\begin{bmatrix}\rho^u_{c\alpha} & \sigma_{c\alpha,c\beta} & \sigma_{c\alpha,c'}\\ \sigma_{c\alpha,c\beta} & \rho^u_{c\beta} & 0\\ \sigma_{c\alpha,c'} & 0 & \rho^u_{c'}\end{bmatrix}\begin{pmatrix}\{\Delta C_z^\alpha(T)\}\\ \{\Delta C_z^\beta(T)\}\\ \{\Delta C_z'(T)\}\end{pmatrix} \quad (10)$$

Note that cross relaxation with proton spins is eliminated by proton saturation, which occurs throughout the relaxation period T. The exact evolution of $\Delta C_z^\alpha(T)$ is multiexponential, with rates which are eigenvalues of the relaxation matrix given in eq 10. To understand the contributions of initial conditions and individual relaxation elements to the relaxation of $\Delta C_z^\alpha(T)$, perturbation theory is appropriate for relatively small values of σ/ρ. To second order,

$$\Delta C_z^\alpha(T) = A_0(T) + A_1(T) + A_2(T)$$

where

(38) Sorenson, O. W.; Eich, G.; Levitt, M. H.; Bodenhausen, G.; Ernst, R. R. *Prog. Nucl. Magn. Reson. Spectrosc.* **1983**, *16*, 163.
(39) Van de Ven, F. J. M.; Hilbers, C. W. *J. Magn. Reson.* **1983**, *54*, 512.
(40) Packer, K. J.; Wright, K. M. *Mol. Phys.* **1983**, *50*, 797.

Table 2. Selected Carbon Relaxation Rates Measured for $^{13}C_3$-Alanine Dissolved in Perdeuterated Glycerol at 10 °C

measured quantity	value (ms)
$1/\rho^{u}_{c'}$ [a]	1823 ± 222
$1/\rho^{u}_{c\alpha}$ [b]	625 ± 7
$1/\rho^{u}_{c\beta}$ [c]	308 ± 2
$1/(\rho^{u}_{c\alpha} + \sigma_{c\alpha,c\beta})$ [d]	737 ± 10
$1/(\rho^{u}_{c\alpha} + \sigma_{c\alpha,c\beta} + \sigma_{c\alpha,c'})$ [e]	1079 ± 20

[a] Measured by selective inversion of the carbonyl (C′) spin using ^{13}C observe spectroscopy. [b] Measured by selective inversion of the C$^{\alpha}$ spin. Magnetization originates on carbon and is detected on H$^{\alpha}$. [c] Measured by selective inversion of the C$^{\beta}$ spin. Magnetization originates on carbon and is detected on H$^{\beta}$. [d] Measured by selective inversion of the C$^{\alpha}$ and C$^{\beta}$ spins. Magnetization originates on carbon and is detected on H$^{\alpha}$. [e] Measured by inversion of the C$^{\alpha}$, C$^{\beta}$, and C′ spins. Magnetization originates on carbon and is detected on H$^{\alpha}$.

$$A_0(T) = \Delta C_z^{\alpha}(0)\exp(-\rho^{u}_{c\alpha}T)$$

$$A_1(T) = [\Delta C_z^{\beta}(0)\sigma_{c\alpha,c\beta}/(\rho^{u}_{c\alpha} - \rho^{u}_{c\beta})]\{\exp(-\rho^{u}_{c\alpha}T) - \exp(-\rho^{u}_{c\beta}T)\} + [\Delta C_z'(0)\sigma_{c\alpha,c'}/(\rho^{u}_{c\alpha} - \rho^{u}_{c'})]\{\exp(-\rho^{u}_{c\alpha}T) - \exp(-\rho^{u}_{c'}T)\}$$

$$\sim -\Delta C_z^{\beta}(0)[\sigma_{c\alpha,c\beta}T - (\sigma_{c\alpha,c\beta}/2)(\rho^{u}_{c\alpha} + \rho^{u}_{c\beta})T^2] - \Delta C_z'(0)[\sigma_{c\alpha,c'}T - (\sigma_{c\alpha,c'}/2)(\rho^{u}_{c\alpha} + \rho^{u}_{c'})T^2]$$

$$A_2(T) = \Delta C_z^{\alpha}(0)[\sigma^2_{c\alpha,c\beta}/(\rho^{u}_{c\alpha} - \rho^{u}_{c\beta})^2\{\exp(-\rho^{u}_{c\beta}T) - \exp(-\rho^{u}_{c\alpha}T)\} + \sigma^2_{c\alpha,c'}/(\rho^{u}_{c\alpha} - \rho^{u}_{c'})^2\{\exp(-\rho^{u}_{c'}T) - \exp(-\rho^{u}_{c\alpha}T)\} - T\exp(-\rho^{u}_{c\alpha}T)\{\sigma^2_{c\alpha,c\beta}/(\rho^{u}_{c\alpha} - \rho^{u}_{c\beta}) + \sigma^2_{c\alpha,c'}/(\rho^{u}_{c\alpha} - \rho^{u}_{c'})\}]$$

$$\sim 0.5\Delta C_z^{\alpha}(0)T^2[\sigma^2_{c\alpha,c\beta} + \sigma^2_{c\alpha,c'}] \qquad (11)$$

For the case of alanine and the sequence of Figure 1a, $\Delta C_z'(0) = 0$. As has been described previously, when the phase $\phi 2$ of the $90_{\phi 2}$-ξ-$90_{\phi 2}$ element in Figure 1d is incremented by 90°, the sign of $\Delta C_z^{\alpha}(0)$ is inverted, while $\Delta C_z^{\beta}(0)$ remains unchanged. Therefore, averaged over a complete phase cycle, where the phase of the receiver is also inverted when $\phi 2$ is incremented, the $A_1(T)$ term will not contribute to the resultant signal, while both $A_0(T)$ and $A_2(T)$ will add constructively to the signal. Assuming that $|\sigma_{c\alpha,c\beta}/\rho^{u}_{c\alpha}| < 0.25$ and $|\sigma_{c\alpha,c'}/\rho^{u}_{c\alpha}| < 0.25$ (i.e., $\tau_c < 18$ ns; see Figure 3), the contribution of $A_2(T)$ to the measured decay of $\Delta C_z^{\alpha}(T)$ at $T = 1/\rho^{u}_{c\alpha}$ is less than $(1/16)\Delta C_z^{\alpha}(0)$ or less than approximately 20% that of $A_0(1/\rho^{u}_{c\alpha})$. That is, if the decay of magnetization is approximated as single exponential, an error in the value of magnetization at $T = 1/\rho^{u}_{c\alpha}$ of less than ~20% is predicted for $|\sigma/\rho| = 0.25$. In order to evaluate the errors that might be expected in measuring $\rho^{u}_{c\alpha}$ from a single exponential fit of the relaxation data for time points extending to $T \leq 1/\rho^{u}_{c\alpha}$, we have measured all the pertinent autorelaxation and cross relaxation rates in alanine. In particular, selective T_1 values of ^{13}C′, ^{13}C$^{\alpha}$, and ^{13}C$^{\beta}$ spins have been measured in uniformly ^{13}C-labeled alanine at 10 °C with experiments where magnetization originates on carbon. Additionally, initial recovery rates of the ^{13}C$^{\alpha}$ spin in uniformly ^{13}C-labeled alanine have been measured for the cases where all of the carbons (^{13}C′, ^{13}C$^{\alpha}$, and ^{13}C$^{\beta}$) are inverted and for the case where only the ^{13}C$^{\alpha}$ and ^{13}C$^{\beta}$ spins are inverted. In all experiments the proton spins were saturated during the relaxation time T. The results of these experiments are presented in Table 2.

Equation 8.1 indicates that in the limit of short relaxation time T,

$$d/dT\{\Delta C_z^{i}(T)\}|_{T=0} = -\rho^{u}_{ci}\Delta C_z^{i}(0) \qquad (12.1)$$

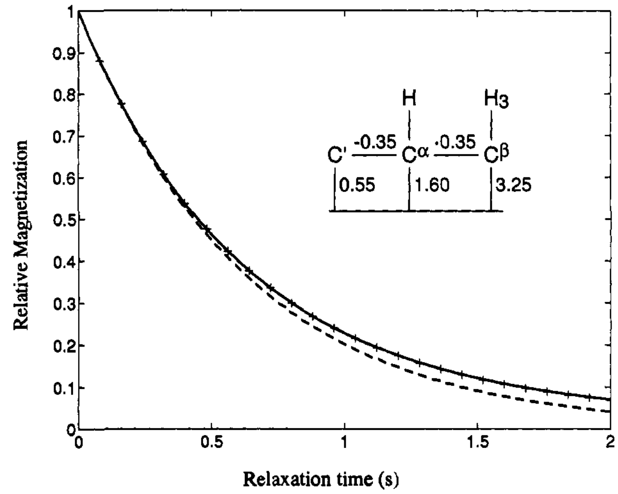

Figure 4. Relative ^{13}C$^{\alpha}$ z magnetization, $\Delta C_z^{\alpha}(T)$, as a function of relaxation time, T, assuming the relaxation rates in the figure. The auto relaxation rates are indicated along vertical lines extending from the appropriate carbon, while cross relaxation rates are listed above horizontal lines connecting the carbon spins. The relaxation rates are based on a series of measurements on alanine dissolved in glycerol at 10 °C, whereby each of the ^{13}C′, ^{13}C$^{\alpha}$, and ^{13}C$^{\beta}$ carbons are inverted selectively, and experiments where either the ^{13}C$^{\alpha}$ and ^{13}C$^{\beta}$ spins are inverted simultaneously or all three carbon spins are inverted together. Cross relaxation rates are extracted from the latter two experiments using second-order perturbation theory (eq 11), which provides a much more reliable estimate of cross relaxation values than a difference of simple exponential fits. The values of $\sigma_{c\alpha,c\beta}$ and $\sigma_{c\alpha,c'}$ were fixed to be the same in the fitting program. The solid line shows the relaxation curve which includes all relaxation pathways, while the broken line indicates the single exponential curve $\exp(-\rho^{u}_{c\alpha}T)$, where $\rho^{u}_{c\alpha} = 1.60$ s^{-1}. Values indicated by the symbol + were calculated using second-order perturbation theory (eq 11) described in the text. Note the excellent agreement between results predicted on the basis of the perturbation treatment and the exact solution obtained via matrix diagonalization (solid line).

$$d/dT\{\Delta C_z^{\alpha}(T)\}|_{T=0} = -\{\rho^{u}_{c\alpha} + \sigma_{c\alpha,c\beta}\}\Delta C_z^{\alpha}(0) \qquad (12.2)$$

$$d/dT\{\Delta C_z^{\alpha}(T)\}|_{T=0} = -\{\rho^{u}_{c\alpha} + \sigma_{c\alpha,c\beta} + \sigma_{c\alpha,c'}\}\Delta C_z^{\alpha}(0) \qquad (12.3)$$

for the cases where only carbon spin i ($i = \alpha, \beta, '$) is inverted (12.1), both ^{13}C$^{\alpha}$ and ^{13}C$^{\beta}$ spins are inverted (12.2), and all spins are inverted (12.3), respectively. In the derivation of eq 12, the assumption that $C_z^{\alpha}(0) = C_z^{\beta}(0) = C_z'(0)$ has been made. This is valid only if the repetition rate between scans is sufficiently slow to allow for complete relaxation and also if the ^{1}H–^{13}C NOE does not build up between scans (which would establish $C_z^{\beta}(0) > C_z^{\alpha}(0) > C_z'(0)$ for the case of alanine). In the case where all carbons are inverted, the initial ^{13}C$^{\alpha}$ relaxation rate in uniformly labeled alanine, $\rho^{u}_{c\alpha} + \sigma_{c\alpha,c\beta} + \sigma_{c\alpha,c'}$, should be very similar to the measured ^{13}C$^{\alpha}$ relaxation rate in the singly labeled population of alanine molecules. This can be understood by recognizing that the $J(0)$ homonuclear ^{13}C–^{13}C spectral density terms in $\rho^{u}_{c\alpha}$ are canceled by equal but opposite in sign $J(0)$ contributions to $\sigma_{c\alpha,c\beta}$ and $\sigma_{c\alpha,c'}$ in the limit of $\omega\tau_c > 1$, so that $\rho^{u}_{c\alpha} + \sigma_{c\alpha,c\beta} + \sigma_{c\alpha,c'} \sim \rho_{c\alpha,H\alpha}$.

The results presented in Table 2 are summarized graphically in Figure 4, where the autorelaxation rates (selective longitudinal relaxation rates) are indicated along the vertical lines and the cross relaxation rates are provided along the horizontal lines. Using the measured values for the autorelaxation and cross relaxation rates, we have examined the sensitivity of the extracted initial ^{13}C$^{\alpha}$ longitudinal relaxation rate to the length of the recovery time, T. Providing that $T \leq 1/\rho^{u}_{c\alpha}$, errors of less than 4% in measured values of $\rho^{u}_{c\alpha}$ are obtained. Figure 4 illustrates that for $T \leq 1/\rho^{u}_{c\alpha}$ (~0.63 s in the present case), reasonable values of $\rho^{u}_{c\alpha}$ can be extracted from single exponential fits of the data. Note that the simulations were performed using relaxation parameters determined for alanine dissolved in glycerol at 10 °C, where a correlation time of ~17 ns was estimated from $T_{1\rho}$ data. The error in measured values of $\rho^{u}_{c\alpha}$ decreases significantly as the value of $|\sigma/\rho|$ drops. For example, for $\tau_c \sim 10$ ns, $|\sigma/\rho| \sim 0.1$, and an error of ~1% is predicted. Also shown in Figure 4 is a comparison of the decay of magnetization predicted using second-order perturbation theory (eq 11) with the exact decay based on the values of ρ and σ reported. Identical relaxation profiles are obtained for the values of T examined ($T \leq \sim 3/\rho^{u}_{c\alpha}$).

The relaxation rate of the alanine $^{13}C^{\beta}$ spin is considerably larger than might be expected for $^{13}C^{\beta}$ nuclei of other amino acids. In order to establish whether differences in $^{13}C^{\beta}$ relaxation rates would significantly influence the measured $^{13}C^{\alpha}$ relaxation times, simulations have been performed using values for the selective relaxation rate of the $^{13}C^{\beta}$ spin that vary by as much as a factor of 5 from the rate reported for the alanine methyl carbon. The results indicate that for $T \leq 1/\rho^{u}_{c\alpha}$, the recovery of $^{13}C^{\alpha}$ magnetization is essentially independent of the rate of recovery of the adjacent $^{13}C^{\beta}$ spin (less than 1% change in $^{13}C^{\alpha}$ relaxation rate for the range of $^{13}C^{\beta}$ spin relaxation rates examined).

To this point, most of our discussion has focused on the measurement of $^{13}C^{\alpha}$ T_1 values in the alanine system. The use of alanine as a test system is to establish the important contributions to the relaxation of ^{13}C spins in uniformly labeled, highly enriched molecules with high signal-to-noise so that accurate measurements on protein samples can be made. The results presented to this point clearly illustrate that, in addition to the major contribution to carbon longitudinal relaxation arising from the directly attached proton spin(s), in macromolecules there is an important contribution from one-bond coupled carbon spins as well. This additional contribution must be taken into account in the interpretation of measured T_1 values in terms of motional properties.

The relaxation behavior of $^{13}C^{\alpha}$ spins in proteins is, in principal, more complicated than that in alanine, since the spin systems involved are in general more complex. In addition to contributions to $^{13}C^{\alpha}$ longitudinal relaxation from adjacent carbon spins, there is the possibility that second-order effects originating from the $^{13}C^{\gamma}$ carbon may make a contribution as well. A second-order perturbation theory calculation shows that for a spin system of arbitrary complexity, the relaxation of a particular carbon spin i is given by

$$\Delta C_z^{\,i}(T) = A_0(T) + A_1(T) + A_2(T)$$

where

$$A_0(T) = \Delta C_z^{\,i}(0)\exp(-\rho^u_{\,i}T)$$

$$A_1(T) = \sum_{j\neq i}[\Delta C_z^{\,j}(0)\sigma_{i,j}/(\rho^u_{\,i} - \rho^u_{\,j})]\{\exp(-\rho^u_{\,i}T) - \exp(-\rho^u_{\,j}T)\}$$

$$\sim \sum_{j\neq i}\Delta C_z^{\,j}(0)\{-\sigma_{i,j}T + 0.5\sigma_{i,j}(\rho^u_{\,i} + \rho^u_{\,j})T^2\}$$

$$A_2(T) = \sum_{j\neq i}\sigma_{i,j}[\sum_{k\neq j\neq i}\{[\Delta C_z^{\,k}(0)\sigma_{j,k}/(\rho^u_{\,j} - \rho^u_{\,k})] \times [\{\exp(-\rho^u_{\,k}T) - \exp(-\rho^u_{\,i}T)\}/(\rho^u_{\,i} - \rho^u_{\,k}) - \{\exp(-\rho^u_{\,j}T) - \exp(-\rho^u_{\,i}T)\}/(\rho^u_{\,i} - \rho^u_{\,j})]\} + [\Delta C_z^{\,i}(0)\sigma_{i,j}/(\rho^u_{\,j} - \rho^u_{\,i})][T \times \exp(-\rho^u_{\,i}T) - \{\exp(-\rho^u_{\,j}T) - \exp(-\rho^u_{\,i}T)\}/(\rho^u_{\,i} - \rho^u_{\,j})]]$$

$$\sim 0.5\sum_{j\neq i}[\Delta C_z^{\,i}(0)\sigma^2_{\,i,j}T^2 + \sum_{k\neq j\neq i}\Delta C_z^{\,k}(0)\sigma_{i,j}\sigma_{j,k}T^2] \qquad (13)$$

In eq 13, spins j are the collection of spins that are one-bond coupled to spin i, and spins k are the collection of spins which are, in turn, one-bond coupled to j ($k \neq i$). For the case of interest here, namely the relaxation of $^{13}C^{\alpha}$ magnetization, $i = {}^{13}C^{\alpha}$, $j = {}^{13}C^{\beta}$ or $^{13}C'$, and $k = {}^{13}C^{\gamma}$.

The pulse sequence used to measure $^{13}C^{\alpha}$ T_1 values in highly enriched, uniformly ^{13}C-labeled proteins is indicated in Figure 1a. Immediately following longitudinal recovery, T (point c), the magnetization can be described by eq 13. Using the first line of the phase cycle indicated in the legend to Figure 1, $\Delta C_z^{\,i}(0)$ ($i = \alpha, \beta, \gamma$) is to be replaced by

$$\Delta C_z^{\,i}(0) = A\sin(2\pi J_{HC}\tau_a)\sin(\pi J_{HC}\tau_b)\cos^n(2\pi J_{CC}\delta) \times \exp(-2\delta/T_{2,Ci})\cos(\omega_{ci}t_1) \qquad (14.1)$$

$$\Delta C_z^{\,i}(0) = A'\sin(2\pi J_{HC}\tau_a)\sin(2\pi J_{HC}\tau_b)\cos^n(2\pi J_{CC}\delta) \times \exp(-2\delta/T_{2,Ci})\cos(\omega_{ci}t_1) \qquad (14.2)$$

$$\Delta C_z^{\,i}(0) = 3A''\sin(2\pi J_{HC}\tau_a)\sin(\pi J_{HC}\tau_b)\cos^2(\pi J_{HC}\tau_b) \times \cos(2\pi J_{CC}\delta)\exp(-2\delta/T_{2,Ci})\cos(\omega_{ci}t_1) \qquad (14.3)$$

for CH (14.1), CH_2 (14.2), and CH_3 (14.3) spin systems where $i = \{\alpha, \beta, \gamma\}$ and n is the number of carbons attached to the particular carbon spin (excluding carbonyl carbons). The coefficients A, A', and A'' depend partly on the relaxation delay between scans and also on the ^1H T_1 values for the appropriate spin system. Alternation of the phase $\phi 1$ by 90° gives identical results with the exception that the $\cos(\omega_{ci}t_1)$ terms in eq 14 are replaced by $-\sin(\omega_{ci}t_1)$ terms. Combination of the resultant data using the recipe of States,[41] followed by two-dimensional Fourier transformation, gives cross peaks at $(\omega_{c\alpha},\omega_{H\alpha})$ with intensity proportional to

$$\Delta C_z^{\,\alpha}(0)\exp(-\rho^u_{\,c\alpha}T) + \sum_{j\neq\alpha}\sigma^2_{\,c\alpha,cj}[[\Delta C_z^{\,\alpha}(0)/(\rho^u_{\,cj} - \rho^u_{\,c\alpha})] \times [T\exp(-\rho^u_{\,c\alpha}T) - \{\exp(-\rho^u_{\,cj}T) - \exp(-\rho^u_{\,c\alpha}T)\}/(\rho^u_{\,c\alpha} - \rho^u_{\,cj})]] \qquad (15.1)$$

where the summation includes $j = {}^{13}C^{\beta}$, $^{13}C'$. Note that because of the application of a carbon pulse followed by a gradient at the start of the sequence, the value of $\Delta C_z^{\,i}(0)$ for carbonyl spins is zero. In addition, for both AX_2 and AX_3 spin systems, the terms $\Delta C_z^{\,i}(0)$ will be quite small since the delays in the sequence are optimized for transfer involving CH ^1H–^{13}C spin systems. For this reason and since $\sigma/\rho < 1$, it is likely that only very weak cross peaks at $(\omega_{c\beta},\omega_{H\alpha})$ and $(\omega_{c\gamma},\omega_{H\alpha})$ will be observed, if at all. (Cross peaks at $(\omega_{c\beta},\omega_{H\alpha})$ are much more likely for isoleucine, threonine, and valine residues, while cross peaks at $(\omega_{c\gamma},\omega_{H\alpha})$ are more likely for leucine owing to the fact that the C^{β} (isoleucine, threonine, and valine) or C^{γ} (leucine) carbon is coupled directly to only a single proton in each of these cases.) The intensities of such cross peaks are proportional to

$$[\Delta C_z^{\,\beta}(0)\sigma_{c\alpha,c\beta}/(\rho^u_{\,c\alpha} - \rho^u_{\,c\beta})]\{\exp(-\rho^u_{\,c\alpha}T) - \exp(-\rho^u_{\,c\beta}T)\}$$

and

$$\sigma_{c\alpha,c\beta}\sum_{\gamma}\{[\Delta C_z^{\,\gamma}(0)\sigma_{c\beta,c\gamma}/(\rho^u_{\,c\beta} - \rho^u_{\,c\gamma})][\{\exp(-\rho^u_{\,c\gamma}T) - \exp(-\rho^u_{\,c\alpha}T)\}/(\rho^u_{\,c\alpha} - \rho^u_{\,c\gamma}) - \{\exp(-\rho^u_{\,c\beta}T) - \exp(-\rho^u_{\,c\alpha}T)\}/(\rho^u_{\,c\alpha} - \rho^u_{\,c\beta})]\} \qquad (15.2)$$

for $(\omega_{c\beta},\omega_{H\alpha})$ and $(\omega_{c\gamma},\omega_{H\alpha})$, respectively. In eq 15.2, the summation is over all the $^{13}C^{\gamma}$ spins.

(41) States, D. J.; Haberkorn, R.; Ruben, D. J. *J. Magn. Reson.* **1982**, *48*, 268.

In order to evaluate whether accurate values of $\rho^{u}_{c\alpha}$ can be extracted from single exponential fits of the intensities of the cross peaks at $(\omega_{c\alpha},\omega_{H\alpha})$ as a function of time, the relative intensities of the first and second terms in eq 15.1 must be compared. Expanding the second term of eq 15.1 and retaining terms of order T^2 and lower gives $[0.5\sum_{j\neq\alpha}\Delta C_z^{\alpha}(0)\sigma^2_{\alpha,j}T^2]$. It is easy to show that for $T \leq 1/\rho^{u}_{c\alpha}$ and assuming $|\sigma_{c\alpha,c'}/\rho^{u}_{c\alpha}| < 0.25$ ($\tau_c < 18$ ns; see Figure 3), the contribution from this term to the intensity of the $(\omega_{c\alpha},\omega_{H\alpha})$ cross peak is less than 20% that of the first term. Numerical simulations show that for $|\sigma_{c\alpha,c'}/\rho^{u}_{c\alpha}| = 0.25$ and $\rho^{u}_{c\alpha} \sim 1.6$ ($\tau_c \sim 18$ ns), errors of no more than 5–6% in measured values of $\rho^{u}_{c\alpha}$ are obtained from single exponential fits of the data. As discussed above, this error decreases significantly as τ_c decreases. Thus, for proteins with $\tau_c < \sim 20$ ns (MW < ~30 kDa), accurate relaxation times, $1/\rho^{u}_{c\alpha}$, can be extracted from cross peak intensities measured as a function of T in exactly the same manner as relaxation times of isolated heteroatoms are determined. In principle, cross relaxation rates can also be determined from these spectra; however, in practice we have not observed the very weak cross peaks in protein applications considered so far.

The experiment for measuring T_1 values that we have just described records the $^{13}C^{\alpha}$ chemical shift prior to the relaxation period, T. At first glance it might be assumed that equivalent experiments could be performed by encoding the carbon chemical shift after the relaxation period. In the latter experiment, magnetization is transferred from $^1H \rightarrow {}^{13}C$ as before, and antiphase carbon magnetization allowed to refocus with respect to the ^1H–^{13}C scalar coupling and carbon magnetization subsequently transferred to the z axis to allow longitudinal relaxation to occur for a time, T. After the delay T, transverse carbon magnetization is generated, and carbon chemical shift is recorded. Note, however, that in this case interpretation of the data is not as straightforward, since all of the terms in eq 13 which contribute to the intensity of cross peak at $(\omega_{ci},\omega_{H\alpha})$ $(i \neq \alpha)$ in the case of the scheme of Figure 1 now contribute to the intensity of the cross peak at $(\omega_{c\alpha},\omega_{H\alpha})$. Consider the measurement of the $^{13}C^{\alpha}$ T_1 values in threonine, isoleucine, or valine residues. These three amino acids have β carbons with only a single attached proton so that both (H^{α},C^{α}) and (H^{β},C^{β}) pairs are heteronuclear CH spin systems. The initial time evolution of $^{13}C^{\alpha}$ z magnetization $(d/dT\{\Delta C_z^{i}(T)\}|_{T=0})$ is given by eq 12.2 since $C_z^{\alpha}(0) = C_z^{\beta}(0)$, neglecting the effects of relaxation prior to the start of the recovery time, T. That is, the initial relaxation rate is given by $\rho^{u}_{c\alpha} + \sigma_{c\alpha,c\beta}$. In contrast, for the remaining amino acids (with the exception of glycine) the (H^{α},C^{α}) pairs constitute CH spin systems with the C^{β} spin associated with either CH_2 or CH_3 spin systems. The inefficient transfer of in-phase proton magnetization to in-phase carbon magnetization for CH_n $(n > 1)$ spin systems using delays optimized for efficient transfer involving CH spin systems implies that $C_z^{\alpha}(0) \gg C_z^{\beta}(0)$. However, depending on the exact magnitudes of the ^1H–^{13}C couplings involved and the delays chosen in the pulse sequence, it may not be possible to completely neglect the initial relaxation contributions from the $\sigma_{c\alpha,c\beta}$ cross relaxation term. In the limiting case where $C_z^{\beta}(0) = 0$, the initial relaxation rate is $\rho^{u}_{c\alpha}$ for these amino acids. Differences in longitudinal relaxation rates of H^{α} and H^{β} spins and transverse relaxation rates of C^{α} and C^{β} magnetization will complicate the extraction of accurate relaxation times further. In contrast, the experiments indicated in Figure 1 provide a measure of heteronuclear relaxation times in a manner which is independent of the initial magnetization states of any spins dipolar coupled to the $^{13}C^{\alpha}$ nucleus. That is, for the case of $^{13}C^{\alpha}$ spins, measurements of relaxation rates from intensities of the cross peaks at $(\omega_{c\alpha},\omega_{H\alpha})$ do not depend on the values of $\Delta C_z^{\beta}(0)$ or $\Delta C_z'(0)$. For this reason the pulse schemes of Figure 1 are preferred.

In summary, the results of this section indicate that for macromolecules, significant contributions to the measured $^{13}C^{\alpha}$ longitudinal relaxation rates arise from adjacent carbon spins. Such contributions can be accounted for in a straightforward manner (see eq 6.1). Providing that $\rho^{u}_{c\alpha}$ values are measured from magnetization that is sampled for times less than $\sim 1/\rho^{u}_{c\alpha}$, for proteins less than ~30 kDa, accurate values of $\rho^{u}_{c\alpha}$ can be extracted from single exponential fits of the relaxation data.

Table 3. Steady-State $^1H^{\alpha}$–$^{13}C^{\alpha}$ NOE Values for Singly (NOE^s) and Uniformly (NOE^u) ^{13}C-Labeled Alanine Dissolved in Perdeuterated Glycerol

T (°C)	NOE^s	NOE^u
40	1.38 ± 0.01	1.38 ± 0.01
30	1.29 ± 0.01	1.29 ± 0.01
20	1.27 ± 0.01	1.31 ± 0.01
10	1.26 ± 0.08	1.46 ± 0.08

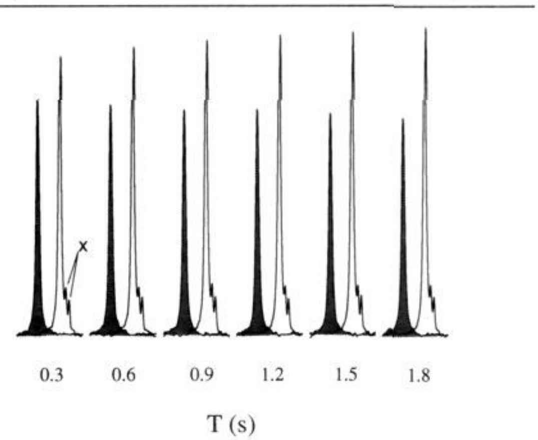

Figure 5. $^{13}C^{\alpha}$ intensity as a function of ^1H saturation time (T) for singly labeled alanine (unshaded lines) and $^{13}C_3$-alanine (shaded lines) recorded using the sequence illustrated in Figure 1c, with region A (between points a and b in the sequence) replaced by the scheme indicated in Figure 1d. The signals from the singly and uniformly labeled population of molecules are shown side-by-side for comparison. In addition to proton saturation, the $^{13}C^{\beta}$ spin was also saturated using a SEDUCE-1[62] decoupling field (4-ms 90° SEDUCE pulses; 138-Hz field at peak height) centered on the $^{13}C^{\beta}$ spin. It is evident that the intensity of $^{13}C^{\alpha}$ magnetization from $^{13}C^{\alpha}$-alanine increases, while the intensity of $^{13}C^{\alpha}$ magnetization from $^{13}C_3$-alanine decreases. The peaks marked with an x are from the glycerol.

(ii) Measurement of the Steady-State $^1H^{\alpha}$–$^{13}C^{\alpha}$ NOE. Table 3 shows the steady-state $^1H^{\alpha}$–$^{13}C^{\alpha}$ NOE values measured for both singly (NOE^s) and uniformly (NOE^u) labeled alanine as a function of temperature. For high temperatures (40 and 30 °C), good agreement between NOE^s and NOE^u is obtained, while the agreement is poor at lower temperatures. The origin of the problem can be understood by recognizing that, at the lower two temperatures where $\tau_c > \sim 6$ ns, saturation of proton spins results in a large enhancement of the $^{13}C^{\beta}$ spin, which builds up efficiently due to the presence of three protons attached to the methyl carbon and the high degree of internal mobility of the methyl group. The enhancement of the $^{13}C^{\beta}$ intensity is transferred via the $^{13}C^{\alpha}$–$^{13}C^{\beta}$ homonuclear NOE to the $^{13}C^{\alpha}$ spin, which therefore shows an increased intensity above and beyond what is expected purely on the basis of the ^1H–^{13}C NOE. Note that the homonuclear carbon–carbon cross relaxation rate increases significantly with increasing correlation time due to the increase in the rate of energy conserving mutual spin flips. In contrast, at the higher temperatures the $^{13}C^{\alpha}$–$^{13}C^{\beta}$ cross relaxation rate $\sigma_{c\alpha,c\beta}$ is sufficiently small (see Figure 3) that this effect is not observed. In order to verify further that this second-order process makes an important contribution to the overall intensity, an experiment in which both the proton spins and the $^{13}C^{\beta}$ spin are saturated was performed at 10 °C, and the results are indicated in Figure 5. The shaded (unshaded) peaks correspond to the signal from the $^{13}C^{\alpha}$ spin in the uniformly (singly) labeled alanine sample. In the case of the singly labeled population of molecules, the intensity of the $^{13}C^{\alpha}$ peak increases as a function of saturation time, as expected. In contrast, the intensity of the $^{13}C^{\alpha}$ signal in uniformly labeled alanine actually decreases. In this case, two competing processes are in effect: (i) the $^{1}H-^{13}C$ NOE, occurring at a rate proportional to $\sigma_{c\alpha,H\alpha}$, which tends to increase the signal as a function of saturation time and (ii) the homonuclear $^{13}C^{\alpha}-^{13}C^{\beta}$ NOE, occurring at a rate proportional to $\sigma_{c\alpha,c\beta}$, which for large molecules is of opposite sign and for the case of $^{13}C^{\beta}$ saturation causes a decrease in the intensity of the $^{13}C^{\alpha}$ signal. Which process dominates depends upon the overall correlation time, since $\sigma_{c\alpha,H\alpha}$ decreases to zero as a function of increasing τ_c, while $\sigma_{c\alpha,c\beta}$ becomes more negative (see Figure 3).

The NOE results from the alanine study suggest that interpretation of $^{1}H^{\alpha}-^{13}C^{\alpha}$ steady-state NOE values in proteins must be made with care because of the influence of $^{13}C^{\alpha}-^{13}C^{\beta}$ cross relaxation. If we consider a $^{13}C^{\alpha}-^{13}C^{\beta}$ carbon fragment with 1 and n protons bound to $^{13}C^{\alpha}$ and $^{13}C^{\beta}$, respectively, it is easy to show that the steady-state $^{1}H^{\alpha}-^{13}C^{\alpha}$ NOE is given by

$$\mathrm{NOE} = 1 + f^{-1}(\sigma_{c\alpha,H\alpha}/\rho^{u}_{c\alpha})\gamma_H/\gamma_c - f^{-1}(\sigma_{c\alpha,c\beta}/\rho^{u}_{c\alpha})n\gamma_H/\gamma_c(\sigma_{c\beta,H\beta}/\rho^{u}_{c\beta}) \quad (16)$$

where $f = 1 - \sigma^{2}_{c\alpha,c\beta}/\rho^{u}_{c\alpha}\rho^{u}_{c\beta}$. Note that $\sigma_{c\alpha,c\beta} < 0$ for $\tau_c > \sim 1.5$ ns. Assuming $n = 1$, $\sigma_{c\alpha,H\alpha} = \sigma_{c\beta,H\beta}$ and $\rho^{u}_{c\alpha} = \rho^{u}_{c\beta}$, for $\sigma/\rho = -0.12$ ($\tau_c = 10$ ns), a value of η = (NOE −1) that is 14% larger than that which would be measured if $\sigma_{c\alpha,c\beta} = 0$ is obtained. If $\tau_c = 18$ ns, this error increases to more than 30%. If the $^{13}C^{\beta}$ position is more mobile than the $^{13}C^{\alpha}$ position (i.e., $\sigma_{c\alpha,H\alpha}/\rho^{u}_{c\alpha} < \sigma_{c\beta,H\beta}/\rho^{u}_{c\beta}$), as is often the case, larger errors are obtained. Without a detailed knowledge of the dynamics at each site *a priori*, it is difficult to predict the contributions from adjacent spins to the measured NOE values.

In principle, the effects of the homonuclear cross relaxation can be minimized or possibly eliminated by recording the carbon intensity as a function of proton saturation time and measuring the initial rate. In practice, we find that for the alanine system (which is the worst case of all the amino acids because of the large $^{1}H^{\beta}-^{13}C^{\beta}$ NOE) even saturation times as low as 100 ms suffer from $^{13}C^{\alpha}-^{13}C^{\beta}$ cross relaxation effects. In the case of proteins, with spectra of much poorer signal-to-noise ratios than for the alanine system considered here and where the $^{1}H^{\alpha}-^{13}C^{\alpha}$ NOE is very small in any event, it seems unlikely that values of sufficient accuracy can be extracted in this manner.

(iii) Measurement of $^{13}C^{\alpha}$ $T_{1\rho}$ Values. Measurement of transverse relaxation time constants provides an important source of motional information since, unlike T_1 and $^{1}H-^{13}C$ NOE measurements (in the absence of carbon–carbon cross relaxation), the dominant term contributing to relaxation is proportional to spectral density functions evaluated at $\omega = 0$.[35] The measurement of T_2 relaxation times in homonuclear coupled spin systems has long been recognized as being problematic, however.[20a–c] Use of the Carr–Purcell–Meiboom–Gill (CPMG) sequence with a repetition rate between successive 180° pulses which is small compared to the difference in chemical shifts between homonuclear coupled spins leads to an echo modulation which is a function of the scalar coupling.[20a–c] In addition, during the intervals between 180° pulses, the signal oscillates between in-phase and antiphase heteronuclear components, which relax at different rates in macromolecules.[42–44] The resultant signal decays, therefore, at a rate which depends on the time between the refocusing pulses. For this reason, it is important that the time between the application of the heteronuclear pulses be short compared to $1/(2J_{HX})$, where J_{HX} is the heteronuclear scalar coupling constant. On the other hand, when the pulse repetition rate is large compared to the shift difference, the echo modulation

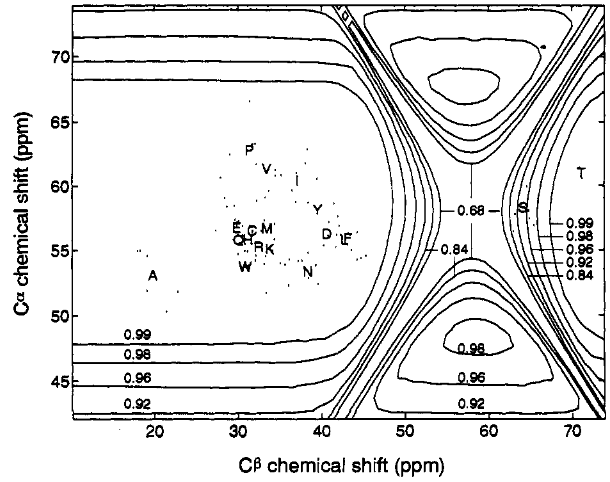

Figure 6. Investigation of the possibility of Hartmann–Hahn transfer during $^{13}C^{\alpha}$ $T_{1\rho}$ measurements. The evolution of $^{13}C^{\alpha}$ magnetization was simulated under the effects of the Hamiltonian indicated in eq 17 in the text. The magnetization was prepared using the $90_{\phi3}$-χ_a-$90_{\phi4}$ scheme described in the text to eliminate chemical shift offset dependencies associated with the projection of magnetization onto the effective field generated by the residual Zeeman field and the spin lock field. A 2-kHz spin lock field applied at 58 ppm was assumed with the effects of rf inhomogeneity and relaxation ignored. $^{13}C^{\alpha}$ magnetization was allowed to evolve for 60 ms, and the ratio of the minimum value in intensity over this time relative to the intensity immediately prior to application of the spin lock was plotted for each $^{13}C^{\alpha}$ and $^{13}C^{\beta}$ position. The $^{13}C^{\alpha}$, $^{13}C^{\beta}$ chemical shifts of the residues in PLCγ1 SH2 complexed with a 12-residue peptide from PDGFR are plotted on the figure. A carbonyl chemical shift of 177 ppm was used in the simulation. The effects of the carbonyl carbon are negligible. Simulations including the $^{13}C^{\gamma}$ carbon indicate that the effects of the $^{13}C^{\gamma}$ carbon are also negligible.

effects discussed in refs 20a–c disappear, but transfer of magnetization between coupled spins in a spin system can occur via the well known Hartmann–Hahn effect.[21] This coherence-transfer process is extremely useful in the identification of amino acid spin systems,[45,46] for example, but significantly complicates the interpretation of relaxation times.

An alternative strategy to the measurement of T_2 values makes use of $T_{1\rho}$ measurements and has been employed extensively by Wagner and co-workers in their studies of protein backbone dynamics via ^{15}N relaxation time measurements.[12,47] While the echo modulation effects which plague the CPMG sequence for slow 180° pulse repetition rates are not important, the possibility of Hartmann–Hahn transfer must be investigated for the measurement of $T_{1\rho}$ values of $^{13}C^{\alpha}$ carbons in uniformly ^{13}C-labeled proteins. The effects of coupling on the evolution of $^{13}C^{\alpha}$ magnetization during application of a spin lock field can be studied by considering a Hamiltonian of the form

$$\mathcal{H} = 2\pi\nu_{c\alpha}C_z^{\alpha} + 2\pi\nu_{c\beta}C_z^{\beta} + 2\pi\nu_{c'}C_z' + 2\pi J_{c\alpha c\beta}C^{\alpha}\cdot C^{\beta} + 2\pi J_{c\alpha c'}C^{\alpha}\cdot C' + 2\pi\nu_1 C_x \quad (17)$$

and asking how magnetization at point c in the sequence of Figure 1b evolves. In eq 17, ν_i is the chemical shift offset from the carrier for spin i, and a spin lock field of strength ν_1 is applied along the x axis. Figure 6 illustrates the results of such a simulation using a 2-kHz spin lock field applied at 58 ppm with the effects of rf inhomogeneity and relaxation ignored. Carbon magnetization, originally prepared with the $90_{\phi3}$-χ_a-$90_{\phi4}$ element, with $\chi_a = 1/(2\pi\nu_1)$ and the 90° pulses assumed to be δ pulses, was allowed to evolve for 60 ms, and the ratio of the minimum value in the intensity of $^{13}C^{\alpha}$ magnetization over this time relative to the intensity immediately prior to application of the spin lock

(42) London, R. E. *J. Magn. Reson.* **1990**, *86*, 410.
(43) Bax, A.; Ikura, M.; Kay, L. E.; Torchia, D. A.; Tschudin, R. *J. Magn. Reson.* **1990**, *86*, 304.
(44) Peng, J. W.; Thanabal, V.; Wagner, G. *J. Magn. Reson.* **1991**, *95*, 421.
(45) Braunschweiler, L.; Ernst, R. R. *J. Magn. Reson.* **1983**, *53*, 521.
(46) Bax, A.; Davis, D. G. *J. Magn. Reson.* **1985**, *65*, 355.
(47) Peng, J. W.; Wagner, G. *J. Magn. Reson.* **1992**, *98*, 308.

Table 4. On-Resonance $^{13}C^{\alpha}$ $T_{1\rho}$ Values for Singly ($T_{1\rho}{}^{s}$) and Uniformly ($T_{1\rho}{}^{u}$) ^{13}C-Labeled Alanine Dissolved in Perdeuterated Glycerol

Temp (°C)	$T_{1\rho}{}^{s}$	$T_{1\rho}{}^{u}$
40	139.7 ± 0.7	135.2 ± 0.6
30	84.0 ± 0.4	81.6 ± 0.1
20	38.9 ± 0.2	37.7 ± 0.1
10	14.6 ± 0.1	14.1 ± 0.2

was plotted for each $^{13}C^{\alpha}$ and $^{13}C^{\beta}$ position. The $^{13}C^{\alpha}$,$^{13}C^{\beta}$ chemical shifts of the residues in PLCγ1 SH2 complexed with a 12-residue phosphopeptide from the platelet-derived growth factor receptor, the protein under study in our laboratory, are plotted on the figure. It is clear that with the exception of serine residues, for which the differences in $^{13}C^{\alpha}$ and $^{13}C^{\beta}$ chemical shifts are reasonably small, Hartmann–Hahn effects can be neglected. Note that the differences in $^{13}C^{\alpha}$ and $^{13}C^{\beta}$ chemical shifts for threonine residues in some proteins may be quite small as well, and it may not be possible to measure accurate $T_{1\rho}$ values in all cases. It is interesting to note that for (fictitious) $^{13}C^{\alpha}$ chemical shifts, less than ~48 ppm or greater than ~68 ppm, the magnetization is modulated slightly over the course of the 60-ms evolution period, even when the attached $^{13}C^{\beta}$ spins resonate as far away as at 15 or 20 ppm. This is not the result of Hartmann–Hahn transfers but rather reflects the fact that at the outset of the spin lock period, the magnetization is no longer aligned parallel to the effective field. As discussed in detail above, for offset values $\nu_{c\alpha}$ that are $\leq\nu_1$, the $90_{\phi3}$-χ_a-$90_{\phi4}$ element in the sequence of Figure 1b "positions" each magnetization component along its appropriate effective field. However, for chemical shift values outside this limit the magnetization is not aligned perfectly with the effective field during the spin lock, resulting in a precession about the (assumed perfectly homogeneous) effective field at a rate given by $\omega_{eff} = [(2\pi\nu_1)^2 + (2\pi\nu_{c\alpha})^2]^{1/2}$. Of course, rf from the present generation of probes is not perfectly homogeneous, leading to the rapid decay of magnetization that is orthogonal to the effective field in real experiments.

Table 4 illustrates the comparison between $^{13}C^{\alpha}$ $T_{1\rho}{}^{s}$ (singly labeled alanine) and $T_{1\rho}{}^{u}$ (uniformly labeled alanine) values measured using a 2-kHz on-resonance rf field with the sequence of Figure 1b at a number of different temperatures. Reasonable agreement is observed at all temperature values. This is perhaps not so surprising since the dominant terms in the expressions for both $T_{1\rho}{}^{s}$ and $T_{1\rho}{}^{u}$ arise from the same effect: dipolar interactions between the $^{13}C^{\alpha}$ spin and the directly coupled ^{1}H spin giving rise to spectral density functions evaluated at $\omega = \omega_{eff} \sim 0$. Note also that the agreement between $T_{1\rho}{}^{s}$ and $T_{1\rho}{}^{u}$ values suggests that Hartmann–Hahn effects in this case are unimportant and that ^{13}C–^{13}C ROE effects can be safely ignored.

Figure 7 compares a $T_{1\rho}$ relaxation profile (unshaded peaks) measured with a 2-kHz spin lock field with a T_2 relaxation time course (shaded peaks) obtained using a CPMG sequence with a spacing between 180° pulses of 500 μs. Results are shown for the $^{13}C^{\alpha}$ spin in uniformly ^{13}C-labeled alanine at 30 °C. The modulation of peak heights as a function of T using the CPMG sequence due to homonuclear scalar coupling is clearly evident.

We conclude the discussion of the $T_{1\rho}$ measurements by noting that our spectra are recorded using a rf field of a single phase rather than a continuous train of 180° pulses of alternating phase.[12,47] Magnetization along the x axis which is on resonance remains locked by a field applied along the $+x$ or $-x$ axis. However, it is easily shown that near resonance, the average Hamiltonian describing the evolution of a spin during the time course of the $[180_x\text{–}180_{-x}]_n$ pulse train for $\nu_1 > \nu_{c\alpha}$ is given by[48]

$$\mathcal{H} = (2/\pi)\omega C_y \tag{18}$$

where ω is the angular offset from the carrier. Thus, the

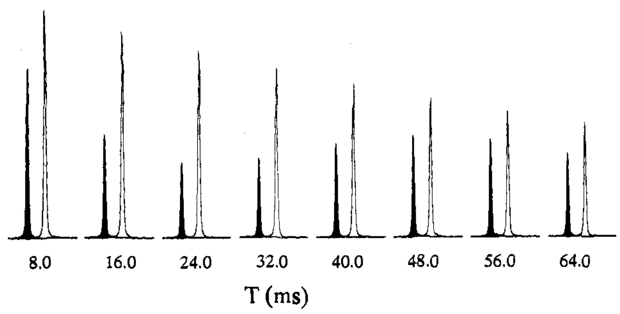

Figure 7. $T_{1\rho}$ (unshaded peaks) or T_2 relaxation (shaded peaks) time course of $^{13}C^{\alpha}$ magnetization from $^{13}C_3$-alanine at 30 °C as a function of the relaxation time T. $T_{1\rho}$ measurements were carried out using an on-resonance, 2-kHz spin locking field, while the T_2 experiment was performed using the CPMG pulse scheme with carbon 180° pulses (7-kHz field) applied every 0.5 ms. In both cases, ^{1}H 180° pulses were applied every 4 ms to eliminate the effects of cross correlation between ^{1}H–^{13}C dipolar and ^{13}C chemical shift anisotropy mechanisms[53,54] or cross correlation effects between ^{13}C–^{13}C and ^{1}H–^{13}C dipolar interactions.

magnetization does not stay locked along the x axis but effectively rotates in the x–z plane, and this complicates the analysis of the data because one must consider the trajectory of the magnetization during the pulse train in order to evaluate spin relaxation properly. Moreover, the intensity of magnetization detected depends not only on the relaxation of the signal but also on the amount precessed in the x–z plane during the time that the field is applied.

(iv) Influence of Other Relaxation Mechanisms on the Measurement of $^{13}C^{\alpha}$ Relaxation Properties. To this point in the manuscript, no mention has been made of the influence of relaxation mechanisms such as chemical shift anisotropy on measured $^{13}C^{\alpha}$ relaxation rates or the dipolar contributions from the adjacent ^{15}N or ^{14}N spins. Straightforward calculations show that a directly bonded ^{15}N (^{14}N) spin (r_{NC} = 1.45 Å[49]) makes a contribution to the longitudinal relaxation rate of a ^{13}C spin of less than 2% (~1%) that of a directly bonded ^{1}H spin (r_{HC} = 1.10 Å[50]), while both ^{15}N and ^{14}N spins make contributions of less than 1% to the transverse relaxation rate of a ^{13}C spin. Assuming a value of $\sigma_{\parallel} - \sigma_{\perp}$ = 25 ppm,[51a,b] the chemical shift anisotropy mechanism contributes less than 1% to the measured longitudinal or transverse relaxation rates of $^{13}C^{\alpha}$ spins. Finally, scalar relaxation of the second kind (^{13}C–^{14}N) makes a negligible contribution to the longitudinal relaxation of the $^{13}C^{\alpha}$ spin, and, for molecules rotating with correlation times in excess of 2 ns, this relaxation mechanism makes a contribution of less than 0.5% to the observed carbon line width. For molecules with correlation times less than ~0.5 ns, the contributions to the carbon line width can become significant. However, $T_{1\rho}$ measurements are, in principle, independent of scalar relaxation effects since, if sufficiently strong spin locking fields are employed, carbon magnetization is locked in the transverse plane while ^{14}N magnetization remains quantized along the z axis. It is straightforward to include these additional relaxation effects in an interpretation of measured relaxation rates in terms of molecular motion. The effects of cross correlation on the measured relaxation rates in highly enriched, uniformly ^{13}C-labeled molecules must also be discussed. The insertion of ^{1}H 180° pulses every several milliseconds (see Figure 1a,b) during the T delay in sequences used to measure T_1 and $T_{1\rho}$ values ensures that interference from cross correlation between chemical shift anisotropy and ^{1}H–^{13}C dipolar interactions[52–54] as well as cross

(48) Hwang, T.; Shaka, A. J. *J. Am. Chem. Soc.* **1992**, *114*, 3157.

(49) (a) Parthasarathy, R. *Acta Crystallogr., Sect. B* **1969**, *25*, 509. (b) Koetzle, T. F.; Hamilton, W. C.; Parthasarathy, P. *Acta Crystallogr., Sect. B* **1972**, *28*, 2083.

(50) Henry, E. R.; Szabo, A. *J. Chem. Phys.* **1985**, *82*, 4753.

(51) (a) Naito, A.; Ganapathy, S.; Akasaka, K.; McDowell, C. A. *J. Chem. Phys.* **1981**, *74*, 3190. (b) Janes, N.; Ganapathy, S.; Oldfield, E. *J. Magn. Reson.* **1983**, *54*, 111.

(52) Boyd, J.; Hommel, U.; Campbell, I. D. *Chem. Phys. Lett.* **1990**, *175*, 477.

Table 5. $^{13}C^{\alpha}$ T_1 Values of Alanine Residues Based on Measurements of $^{13}C^{\alpha}$-Alanine SNase and Uniformly $^{13}C,^{15}N$-Labeled SNase[a]

residue	T_1^{calc}	T_1^{expt}
A1	672	611
A12	709	684
A17	658	631
A58	664	630
A60	644	652
A69	671	669
A90	711	683
A94	693	671
A102	676	635
A109	668	651
A112	691	676
A130	683	698
A145	341	344

[a] In order to compare the $^{13}C^{\alpha}$ T_1 values from singly and uniformly labeled samples, the values of S^2 and τ_e given in ref 55 and calculated using the model-free approach[56a,b] from $^{13}C^{\alpha}$ T_1, T_2, and NOE data measured from the singly labeled sample have been used to calculate the expected T_1 values in a uniformly ^{13}C-labeled sample (T_1^{calc}). Note that in ref 55, a value of 1.09 Å was used for the $^1H^{\alpha}$–$^{13}C^{\alpha}$ bond length; hence this value was used in the calculation. $^{13}C^{\alpha}$ T_1 values for alanine residues measured from the uniformly $^{13}C,^{15}N$-labeled sample are indicated in the column labeled by T_1^{expt}. Errors of approximately 5–7% are reported for the $^{13}C^{\alpha}$ T_1 values measured from the singly labeled sample, and errors of approximately 2–3% are obtained for T_1 values measured on the uniformly labeled sample. Data from residue A132 are not reported because of a ridge of noise that obscures this resonance in all spectra of the uniformly labeled sample. In the derivation of T_1^{calc}, the contribution from the one-bond coupled ^{15}N spin was not included. The contribution from the ^{15}N spin decreased T_1^{calc} by ~2%.

correlation effects between ^{13}C–^{13}C and ^1H–^{13}C dipolar interactions is eliminated. It seems unlikely that cross correlation between carbon–carbon dipolar interactions is significant since similar $T_{1\rho}$ values were obtained in both singly and uniformly labeled alanine molecules at all temperatures and, in addition, the $^{13}C^{\alpha}$ $\rho^{s}_{c\alpha}$ value (measured for the singly labeled alanine sample) and the measured value for $\rho^{u}_{c\alpha} + \sigma_{c\alpha,c\beta} + \sigma_{c\alpha,c'}$ (uniformly labeled sample) are very similar, as expected in the absence of cross correlation. Moreover, measurement of the initial decay rates in all experiments should ensure that the influence of cross correlation effects is kept small.

(v) Application to Proteins. Analysis of relaxation data is most straightforward under the assumption of isotropic motion. Additional degrees of motional freedom can complicate the interpretation of the relaxation data in terms of motional parameters. In uniformly labeled proteins, the value $\rho^{u}_{c\alpha}$ is comprised of dipolar contributions from H^{α}, C^{β}, and C′ spins, and it is possible that each contribution may be modulated to some extent by different motions. For example, consider rotation about the C^{α}–C′ bond. Such motion may contribute to the dipolar relaxation of the $^{13}C^{\alpha}$ nucleus from adjacent $^1H^{\alpha}$ and $^{13}C^{\beta}$ spins, while the $^{13}C^{\alpha}$–$^{13}C'$ dipolar interaction would be unaffected. If this were the case, the functional form of the spectral density functions in eq 6 would have to be modified to reflect this additional motion. Note, however, that even for τ_c values as large as ~17 ns, the dominant term in the relaxation of the $^{13}C^{\alpha}$ spin arises from the $^1H^{\alpha}$–$^{13}C^{\alpha}$ dipolar interaction (see Table 1), and, therefore, to a good first approximation, the value of $\rho^{u}_{c\alpha}$ reports on the dynamics of the H^{α}–C^{α} bond vector. In this context, the excellent agreement between experimental and calculated values of $\{1/T_1^{u} - 1/T_1^{s}\}$ presented in Table 1 indicates that the assumption of isotropic motion is reasonable, at least in the case of alanine dissolved in glycerol.

In order to investigate this further in the context of protein applications, we have measured $^{13}C^{\alpha}$ T_1 values in uniformly

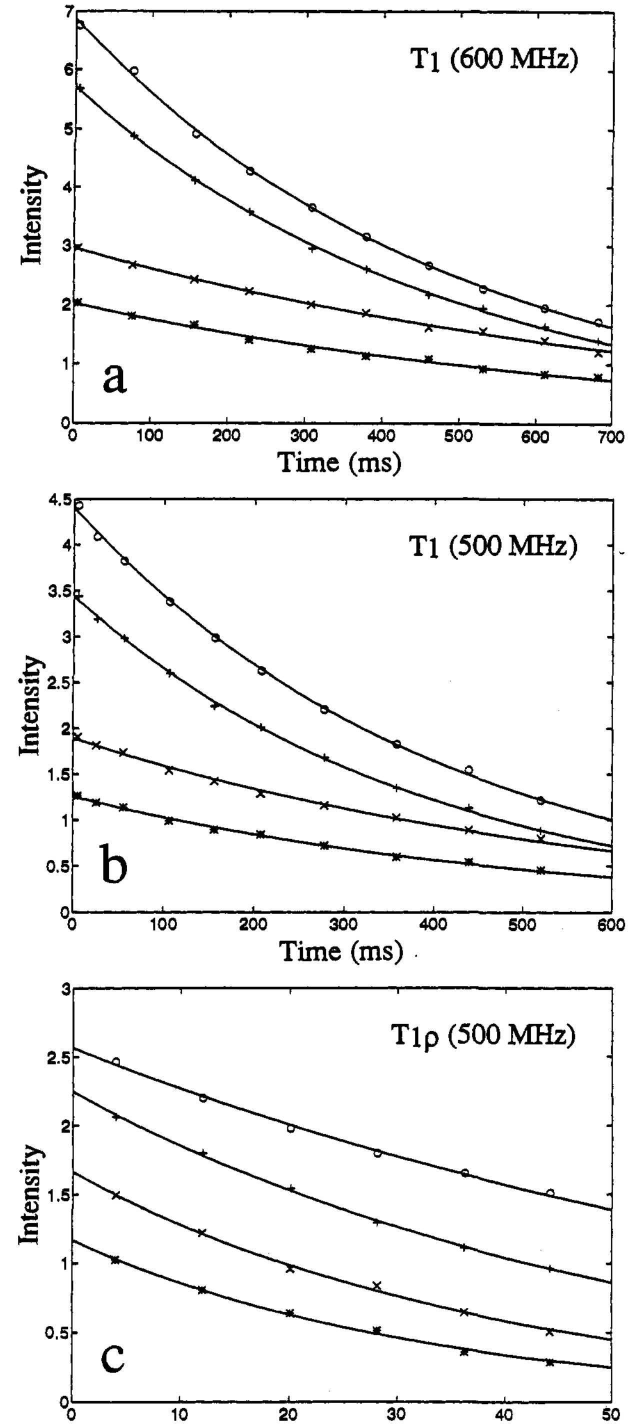

Figure 8. Experimental T_1 (a, b) and $T_{1\rho}$ (c) relaxation data for residues P3, Q61, N71, and E102 measured at 600 (a) and 500 MHz (b, c). The solid curves are the best fits of the data, while the experimental data points are indicated by O (P3), * (Q61), × (N71), and + (E102).

$^{13}C,^{15}N$-labeled staphylococcal nuclease complexed with the ligands Ca^{2+} and thymidine 3′,5′-biphosphate (SNase, MW 18 kDa) and compared these values with results obtained from measurements on a sample labeled specifically with ^{13}C in the C^{α} position of alanine residues. Using the values of S^2 and τ_e that Nicholson et al.[55] have calculated using the model-free approach[56a,b] from $^{13}C^{\alpha}$ T_1, T_2, and NOE values measured from the singly labeled $^{13}C^{\alpha}$-alanine sample, the $^{13}C^{\alpha}$ T_1 values that

(53) Kay, L. E.; Nicholson, L. K.; Delaglio, F.; Bax, A.; Torchia, D. A. *J. Magn. Reson.* **1992**, *97*, 359.
(54) Palmer, A. G.; Skelton, N. J.; Chazin, W. J.; Wright, P. E.; Rance, M. *Mol. Phys.* **1992**, *75*, 699.
(55) Nicholson, L. K.; Kay, L. E.; Torchia, D. A. Manuscript in preparation.
(56) (a) Lipari, G.; Szabo, A. *J. Am. Chem. Soc.* **1982**, *104*, 4546. (b) Lipari, G.; Szabo, A. *J. Am. Chem. Soc.* **1982**, *104*, 4559.

would be expected in a uniformly labeled sample have been calculated using eq 6 and compared directly with the $^{13}C^{\alpha}$ T_1 values measured from the uniformly labeled sample. Table 5 shows that good agreement is obtained. Note that the comparison involving residues A1 and A145 is somewhat suspect since the terminal residues of SNase are disordered and undergo motions that are difficult to characterize using the model-free approach.[55]

The pulse sequences that have been described above have also been applied to measure $^{13}C^{\alpha}$ relaxation times for the C-terminal SH2 domain of PLC-γ1 (105 amino acids) complexed with a 12-residue phosphopeptide from the platelet-derived growth factor receptor (PDGFR). Figure 8 illustrates T_1 results obtained for residues P3, Q61, N71, and E102 at 500 and 600 MHz and $T_{1\rho}$ values at 500 MHz. Because of the difficulties with measuring accurate steady-state (or transient) $^{1}H^{\alpha}$–$^{13}C^{\alpha}$ NOE values, we prefer to measure T_1 relaxation times at a number of different field strengths in order to obtain motional properties of the molecule under study. Relaxation data recorded at 500 and 600 MHz are currently under analysis. The overall goal in this project is to investigate the side-chain dynamics of the protein and how such dynamics change upon binding of peptide. This will require measurement of ^{13}C relaxation times in AX_2 and AX_3 spin systems, where the effects of cross correlation between ^{1}H–^{13}C dipolar interactions are significant.[57a,b] While such effects have been shown to complicate the extraction of accurate relaxation times, pulse schemes do exist for carbon relaxation measurements in AX_3 spin systems.[58,59] In order to obtain relaxation times using two-dimensional polarization-transfer experiments which are consistent with values measured via ^{13}C direct observation methods, it is necessary to ensure that magnetization from each carbon multiplet component be transferred back equally to observable proton magnetization.[59] Given that individual multiplet components can have significantly different transverse relaxation times, it seems unlikely that such a requirement can be satisfied in experiments where the carbon evolution time is recorded using a constant time approach, as is described here. Unfortunately, sensitivity requirements dictate that for measurement of accurate relaxation times in most proteins, highly enriched, ^{13}C-labeled samples must be employed. This, in turn, requires the use of constant time spectroscopy to obtain adequate resolution. Recently Kushlan and LeMaster[60] suggested an elegant solution to the problem whereby $^{13}CH_n$ ($n > 1$) spin systems are converted into $^{13}CHD_{n-1}$ spin systems via deuteration. Cross correlation effects between ^{1}H–^{13}C and ^{2}H–^{13}C dipolar interactions can be eliminated by the application of ^{1}H 180° pulses during the T delay in sequences used to measure relaxation properties in much the same way that the effects of cross correlation between ^{13}C–^{13}C and ^{1}H–^{13}C dipolar interactions are eliminated. Moreover, the influence of cross correlation between ^{2}H–^{13}C dipoles on the relaxation of carbon spins is much less severe than the effects of ^{1}H–^{13}C dipoles, since the gyromagnetic ratio of ^{2}H is only $\sim 1/7$ that of ^{1}H. The use of 50% random deuteration coupled with a high level of ^{13}C enrichment seems like a promising strategy for the study of side-chain dynamics in proteins. We are currently investigating this possibility.

In summary, in this paper we have described a number of experiments for measuring $^{13}C^{\alpha}$ dynamics in highly enriched, uniformly ^{13}C-labeled proteins. Both theory and experiment indicate that the effects of neighboring carbon spins cannot be neglected in the interpretation of ^{13}C T_1 or steady-state $^{1}H^{\alpha}$–$^{13}C^{\alpha}$ NOE data. This does not prohibit the measurement of accurate $^{13}C^{\alpha}$ selective T_1 values, however, providing that only initial decay rates are measured. While carbon–carbon homonuclear couplings do interfere with the measurement of T_2 values using the CPMG sequence, accurate $T_{1\rho}$ measurements can be made for $^{13}C^{\alpha}$ nuclei of all amino acids with the exception of serine residues and in some cases threonine residues, which have nearly identical $^{13}C^{\alpha}$ and $^{13}C^{\beta}$ chemical shifts. Based on the results discussed in this paper, we propose a strategy for measuring accurate $^{13}C^{\alpha}$ motional properties whereby $^{13}C^{\alpha}$ T_1 values are measured using at least two different magnetic field strengths, while $^{13}C^{\alpha}$ $T_{1\rho}$ values are recorded at a single field. The extraction of $^{13}C^{\alpha}$ relaxation times using the proposed strategy will provide a powerful approach for investigating backbone dynamics.

Acknowledgment. Toshio Yamazaki is the recipient of a Human Frontiers Science Program Fellowship. The authors are grateful to Dr. Steve Pascal for providing the $^{13}C^{\alpha}$ and $^{13}C^{\beta}$ chemical shifts for PLC-γ1 SH2, Mr. Alex Singer for preparation of the SH2 sample used in the present study, and Dr. S. Shoelson, Harvard University, for the gift of pY1021 phosphopeptide. The authors would like to thank Dr. Dennis A. Torchia, National Institutes of Health, Bethesda, MD, for many useful discussions and a critical reading of this manuscript. The sample of SNase used in this work was kindly provided by Drs. D. A. Torchia and L. K. Nicholson. This work was supported through grants from the National Sciences and Engineering Research Council of Canada and the National Cancer Institute of Canada with funds from the Canadian Cancer Society.

(57) (a) Werbelow, L. G.; Grant, D. M. *Adv. Magn. Reson.* **1977**, *9*, 536. (b) Kay, L. E.; Torchia, D. A. *J. Magn. Reson.* **1991**, *95*, 536.

(58) Palmer, A. G.; Wright, P. E.; Rance, M. *Chem. Phys. Lett.* **1991**, *185*, 41.

(59) Kay, L. E.; Bull, T. E.; Nicholson, L. K.; Griesinger, C.; Schwalbe, H.; Bax, A.; Torchia, D. A. *J. Magn. Reson.* **1992**, *100*, 538.

(60) Kushlan, D. M.; LeMaster, D. M. *J. Am. Chem. Soc.* **1993**, *115*, 11026.

(61) Shaka, A. J.; Keeler, J.; Frenkiel, T.; Freeman, R. *J. Magn. Reson.* **1983**, *52*, 335.

(62) McCoy, M.; Mueller, L. *J. Am. Chem. Soc.* **1992**, *114*, 2108.

(63) Boyd, J.; Scoffe, N. *J. Magn. Reson.* **1989**, *85*, 406.

(64) Patt, S. L. *J. Magn. Reson.* **1992**, *96*, 94.

(65) Marion, D.; Ikura, M.; Tschudin, R.; Bax, A. *J. Magn. Reson.* **1989**, *85*, 393.